Macromolecules **1992,** *25,* 271–285

Rheological Behavior of Homogeneous Poly(α-methylstyrene)-*block*-polystyrene Copolymers

Jin Kon Kim and Chang Dae Han*

Department of Chemical Engineering, Polytechnic University, Brooklyn, New York 11201

Received October 25, 1990; Revised Manuscript Received August 14, 1991

ABSTRACT: A series of poly(α-methylstyrene)-*block*-polystyrene (PαMS-PS) copolymers having molecular weights ranging from 120 000 to 250 000 and different block length ratios were synthesized via anionic polymerization. Oscillatory shear flow properties of these block copolymers were measured using a Rheometrics mechanical spectrometer at temperatures ranging from 116 to 251 °C, depending on the block copolymer composition. We have concluded that these block copolymers are *homogeneous* as determined by differential scanning calorimetry and, also, by logarithmic plots of dynamic storage modulus versus dynamic loss modulus. This conclusion is further supported by the fact that temperature–frequency superposition gives rise to temperature-independent master curves for the block copolymers. In view of the fact that the block copolymers synthesized must be regarded as entangled homogeneous block copolymers, using the concept of the tube model we have modified on an ad hoc basis the Stockmayer–Kennedy molecular viscoelasticity theory which was developed on the basis of the Rouse theory. The predicted zero-shear viscosities of the PαMS-PS diblock copolymers are compared with experimental results.

Introduction

In 1974 Robeson and co-workers[1] reported on an experimental investigation of phase separation in poly(α-methylstyrene)-*block*-polystyrene (PαMS-PS) copolymers. They determined glass transition temperatures from dynamic mechanical measurements and concluded that microphase separation did not occur until the molecular weight of each block exceeds about 2×10^5. Subsequently, Krause and co-workers[2,3] also investigated phase separation in PαMS-PS diblock copolymers, as well as PS-PαMS-PS and PαMS-PS-PαMS triblock copolymers, by determining glass transition temperatures via differential scanning calorimetry (DSC), and basically confirmed what Robeson et al.[1] had reported earlier. In these studies the appearance of two glass transition temperatures (T_g), one corresponding to the T_g of PS and the other corresponding to the T_g of PαMS, was taken as an indication of microphase separation.

In spite of the fact that over the past three decades numerous studies have been reported on the rheological behavior of block copolymers of styrene and butadiene, and block copolymers of styrene and isoprene, little has been reported on the rheological behavior of block copolymers of α-methylstyrene and styrene. In 1975 Hansen and Shen[4] synthesized a series of PS-PαMS-PS and PαMS-PS-PαMS triblock copolymers and calculated the maximum relaxation times of the block copolymers from stress relaxation experiments. Hansen and Shen specifically chose a range of molecular weights (below 1.5×10^5) that gave rise to *homogeneous* block copolymers, in order to test a molecular viscoelasticity theory that they had developed earlier.[5] They confirmed from the observation made of a single peak of loss tangent that the block copolymers synthesized were indeed homogeneous. In comparing measured maximum relaxation times with theory, Hansen and Shen[4] assumed that their block copolymers were in the Rouse regime although the molecular weight of each block was far greater than the entanglement molecular weight M_e (ca. 1.8×10^4 for PS and 1.35×10^4 for PαMS). It should be pointed out that in Hansen–Shen's study, no viscoelastic properties other than the maximum relaxation times were either measured or calculated. Since the 1975 study of Hansen and Shen, there has been no experimental study reported on the rheological behavior of block copolymers of α-methylstyrene and styrene.

Very recently, we synthesized, via anionic polymerization, a series of *homogeneous* PαMS-PS block copolymers and measured their dynamic viscoelastic properties, namely, the dynamic storage modulus and dynamic loss modulus as functions of angular frequency, at temperatures ranging from 116 to 251 °C, depending on the block copolymer composition. In this paper we shall report on our experimental results and interpret them through a modification of the Stockmayer–Kennedy theory.[6]

Experimental Section

Preparation of PαMS-PS Diblock Copolymers. A series of PαMS-PS diblock copolymers were synthesized via anionic polymerization, using an inert gas, stirred-tank reactor system, very similar to that as described by Hellstern et al.[7] Figure 1 gives a schematic of the reactor system used in this study.[8] Before beginning polymerization, we had to purify argon gas, styrene monomer, α-methylstyrene monomer, and tetrahydrofuran (THF) used as the solvent. Specifically, an ultrapure argon (99.999%, Union Carbide Co.) was purified further by passing through a column which contained a copper-based catalyst (BASF) to remove any trace of oxygen. This oxygen-free argon was then passed through two columns of molecular seives of 40 nm to remove any trace of moisture. By using a two-way teflon valve, the polymerization reactor system was first evacuated and then purged with the purified argon gas. The inhibitor in styrene monomer (99% purity) was removed by passing it through an inhibitor removal column (DTR-7, Scientific Polymer Products Inc.) using a dropping funnel, after which the styrene was poured into a bottle which contained molecular sieves of 40 nm. A few days before polymerization, the styrene monomer was distilled in the presence of CaH_2 at 30 °C, and the middle fraction was received via a two-way teflon stopcock into a flask, where dibutylmagnesium (1.0 M solution in heptane, Aldrich Chemical Co.) had been added. Just before polymerization, the styrene monomer containing dibutylmagnesium was distilled again and the middle fraction of styrene monomer was received directly into the dropping funnel. Purification procedures employed for α-methylstyrene were essentially the same as described above for styrene monomer, except that a slightly higher temperature (36 °C) was used. THF (HPLC grade, Aldrich Chemical Co.) was distilled and refluxed over sodium/benzophenone for 3–4 days to give it a deep purple color, which was an indication of oxygen and moisture absence in the glassware. Just before polymerization, THF was distilled once again in the presence of purified argon and then directly transferred into the reactor,

0024-9297/92/2225-0271$03.00/0

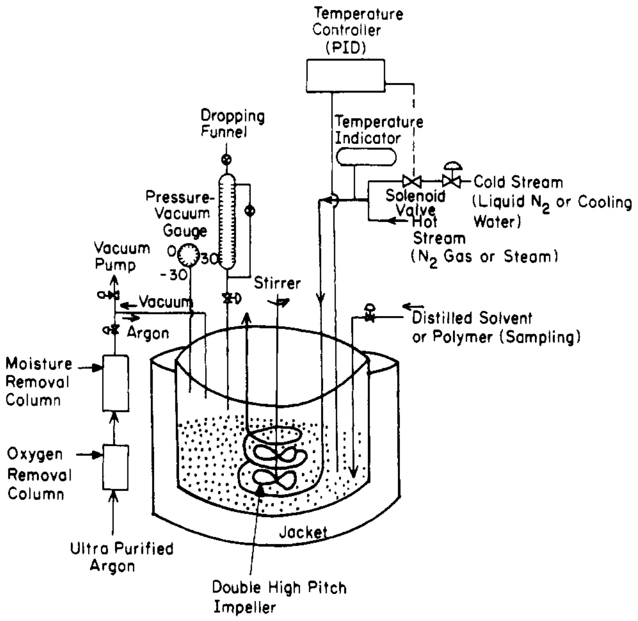

Figure 1. Schematic describing the reactor system employed for anionic polymerization.

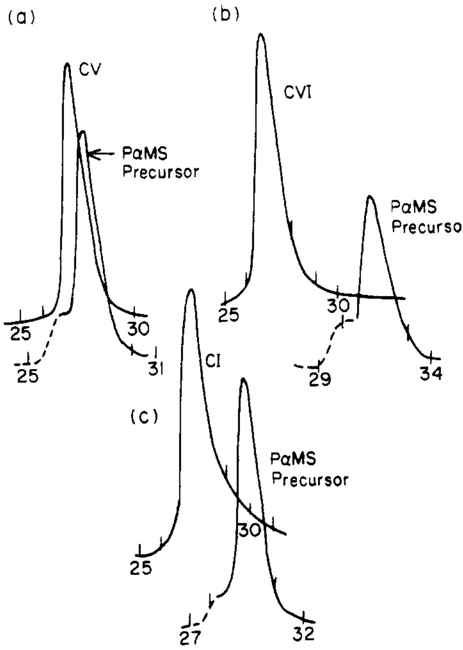

Figure 2. Traces of the GPC chromatogram for PαMS-PS diblock copolymers: (a) sample CV, (b) sample CVI, and (c) sample CI. Also shown are traces of GPC chromatogram for PαMS precursor which was siphoned out just before copolymerization reaction began. The numbers on the chromatograms denote the retention volume (mL).

using a double-end deflected needle (Ace Glass Co.). *sec*-Butyllithium (*sec*-BuLi) (1.3 M in hexane, Aldrich Chemical Co.) was used as the catalyst, as received.

In the polymerization, the reactor was first thoroughly washed with purified THF, then evacuated using high vacuum for 12 h, and finally heated with a heat gun. When the reactor was cool, the distilled THF and α-methylstyrene were added into the reactor, using double-end deflected needles. The reactor was then quickly put under an ultrapure argon atmosphere (ca. 10 psig). After the solution was cooled in the reactor to −70 °C, using a specially designed low-temperature solenoid valve, a very small amount of initiator was added drop by drop, using a hypodermic syringe with a capacity of 0.25 cm^3, in order to remove any impurity that might still be present in the reactor wall, solvent, and α-methylstyrene monomer. We found that when all impurities were removed, the color of the solution in the reactor turned into a bright red. At this point, a predetermined amount of initiator, *sec*-BuLi, was added using a syringe with a capacity of 1.0 cm^3. The reaction for poly(α-methylstyrene) lasted for about 6 h. The "living" poly(α-methylstyrene) was then copolymerized with styrene monomer to form a PαMS-PS diblock copolymer.

Before copolymerization, a small amount of PαMS was siphoned off from the reactor as precursor, which was later used to determine, via gel permeation chromatography (GPC), the molecular weight of PαMS in the synthesized PαMS-PS diblock copolymer. After the sampling of PαMS precursor, styrene monomer in the calibrated dropping funnel was slowly added to the reactor. In the beginning, the color in the reactor changed from deep red to yellowish-orange. When the entire amount of styrene monomer was added, the color gradually returned to deep red. The reaction for the copolymerization lasted about 3 h. Upon completion of the copolymerization reaction, a small amount of degassed methanol was injected into the reactor using a hypodermic syringe to deactivate anions in the reactor, at which point the color of the solution in the reactor changed from deep red to white. Then, the reactor temperature was raised to room temperature, and the solution in the reactor was precipitated by addition of an excess amount of methanol. The precipitated polymer was filtered and dried for 2 days at room temperature under vacuum and finally dried at 90 °C for 12 h under vacuum.

Characterization of PαMS-PS Diblock Copolymers. The molecular weight and molecular weight distribution of PαMS precursor and PαMS-PS diblock copolymers synthesized were determined using a Waters gel permeation chromatograph (GPC) attached with four ultrastyrogel columns (500, 10^3, 10^4, and 10^5). The solvent used was HPLC-grade THF, and the column temperature was kept at 25 ± 1 °C. The GPC chromatogram was calibrated with 10 monodisperse standards of known molecular weights (2×10^3 to 2×10^6) purchased from Scientific Polymer Products, Inc., and poly(α-methylstyrene) standards purchased from the Polyscience Co. We found that the peak retention volumes of PS and PαMS were essentially the same for molecular weights ranging from 4×10^4 to 1.2×10^5, and that for higher molecular weights, the molecular weight of PαMS was found to be slightly higher than that of PS at a given retention volume. The molecular weights of the block copolymers synthesized were determined using the following procedures: (1) Using the calibration curve for homopolymer PαMS, the molecular weight $M_{w,P\alpha MS(b)}$ of PαMS precursor (i.e., PαMS block in a PαMS-PS diblock copolymer) was determined, from which the weight fraction $w_{P\alpha MS}$ of PαMS block in the PαMS-PS diblock copolymer was determined from

$$w_{P\alpha MS} = M_{w,P\alpha MS(b)}/M_{w,P\alpha MS\text{-}PS} \quad (1)$$

where $M_{w,P\alpha MS\text{-}PS}$ is the molecular weight of PαMS-PS diblock copolymer which is yet to be determined. (2) From the measurement of retention volume of a block copolymer sample, together with calibration curves for homopolymers PS and PαMS, respectively, we calculated the molecular weight $M_{w,PS}^*$ of homopolymer PS having the same molecular weight as that of the block copolymer itself, and, also, molecular weight $M_{w,P\alpha MS}^*$ of homopolymer PαMS having the same molecular weight as that of the block copolymer itself. Since the value of $M_{w,P\alpha MS\text{-}PS}$ must lie between the two values, $M_{w,PS}^*$ and $M_{w,P\alpha MS}^*$, we have the relationship:

$$M_{w,P\alpha MS\text{-}PS} = w_{PS}M_{w,PS}^* + w_{P\alpha MS}M_{w,P\alpha MS}^* \quad (2)$$

where $w_{PS} + w_{P\alpha MS} = 1$. In the present study we found that in the range of molecular weight of PαMS-PS diblock copolymers synthesized, the calibration curve obtained for PS using monodisperse standards was *almost* identical to that obtained for PαMS using monodisperse standards.[8] Therefore, we determined values for $M_{w,P\alpha MS\text{-}PS}$ and $w_{P\alpha MS}$ using eqs 1 and 2. Finally, the molecular weight $M_{w,PS(b)}$ of the PS block in the block copolymer was determined from

$$M_{w,P\alpha MS\text{-}PS} = M_{w,P\alpha MS(b)} + M_{w,PS(b)} \quad (3)$$

Figure 2 gives, for illustration purposes, GPC traces for block copolymer samples CI, CV, and CVI. A summary of the molecular weights and molecular weight distributions determined

Table I
Summary of the Molecular Characteristics of the PαMS-PS Block Copolymers and Homopolymers Synthesized

	homopolymer or PαMS block		block copolymer PαMS-PS		GPC	NMR
sample code	$M_w \times 10^{-3}$	M_w/M_n	$M_w \times 10^{-3}$	M_w/M_n[a]	PαMS: wt %[b]	PαMS: wt %
BII	52	1.06	52–70	1.08	43 (45)	47
CI	54	1.06	54–94	1.08	36 (40)	41
CII	99	1.07	99–145	1.09	41 (46)	48
CIII	135	1.07	135–120	1.09	53 (59)	57
CIV	50	1.08	50–130	1.08	27 (29)	28
CV	122	1.06	122–26	1.06	83 (83)	81
CVI	21	1.07	21–167	1.09	11 (11)	13
PS-50	59	1.05			0.0	
PS-200	195	1.07			0.0	
PαMS-50	67	1.06			100	
PαMS-75	80	1.07			100	
PαMS-100	98	1.07			100	

[a] Without including the dead PαMS homopolymer present. [b] The number inside the parentheses includes the dead homopolymer PαMS present in the block copolymer sample.

for the homopolymers and PαMS-PS diblock copolymers synthesized in this study is given in Table I. It can be seen in Figure 2 that the GPC chromatograms for samples CV and CVI have a single peak, indicating a termination-free polymerization, while the GPC chromatogram for sample CI has a shoulder at a position corresponding to the molecular weight of the PαMS precursor. It should be mentioned that the area near the shoulder in the GPC chromatogram for sample CI represents the amount of dead homopolymer PαMS, which resulted from a partial loss of poly(α-methylstyryllithium) anions, in the block copolymer sample. We calculated the weight fraction of dead homopolymer PαMS in each block copolymer sample. The values inside the parentheses of column 6 in Table I represent the weight fraction of PαMS, including the dead homopolymer PαMS present in each block copolymer sample. Notice in Figure 2 that the GPC chromatogram for PαMS precursor has a secondary peak designated by a broken curve at the retention volume corresponding to twice the molecular weight of the main peak. On the other hand, such a secondary peak is not observed in the GPC chromatograms for the block copolymer samples. Therefore, we believe that the secondary peak appearing in the GPC chromatogram for PαMS precursor resulted from the coupling reaction between the "living" anions and CO_2 present in the air,[9] that might have taken place during sampling. It should be pointed out that the values of polydispersity, M_w/M_n, given in column 5 of Table I do not include the dead homopolymer PαMS present in each block copolymer sample. It can be seen in Table I that both homopolymers and block copolymers synthesized in this study can be regarded as nearly monodisperse.

We employed, also, nuclear magnetic resonance (NMR) spectroscopy (Varian T-60) to determine the weight fraction of the PαMS block in PαMS-PS diblock copolymer. For the measurements all samples were dissolved in $CDCl_3$ (10 wt % solid) using 1,4-dioxane as the standard material. Note that TMS overlaps one of the α-methylstyrene peaks. Traces of typical NMR spectra for PS, PαMS, and three PαMS-PS diblock copolymers are given in Figure 3. A major difference in NMR spectrum between PαMS and PS is that for PαMS there are three additional peaks located between 0.8 and −0.8 ppm (based on TMS scale), representing mm (~0.8 ppm), mr (~0.1 ppm), and rr (−0.8 ppm) triads for the three hydrogens in the α-methyl position of PαMS. The weight fractions of mm, mr, and rr triads are 0.14, 0.46, and 0.40, respectively. Using calibration curves the weight fraction of PαMS in a PαMS-PS diblock copolymer can be determined,[3,4] the results of which for the seven block copolymers synthesized for this study are given in the last column of Table I. It should be mentioned that the weight fraction of PαMS determined from NMR includes the dead homopolymer PαMS present in the block copolymer sample. A comparison of the values inside the parentheses of column 6 with those in the last column of Table I indicates to us that two different experimental techniques, GPC and NMR, give rise to essentially the same weight fraction of PαMS in each block copolymer sample.

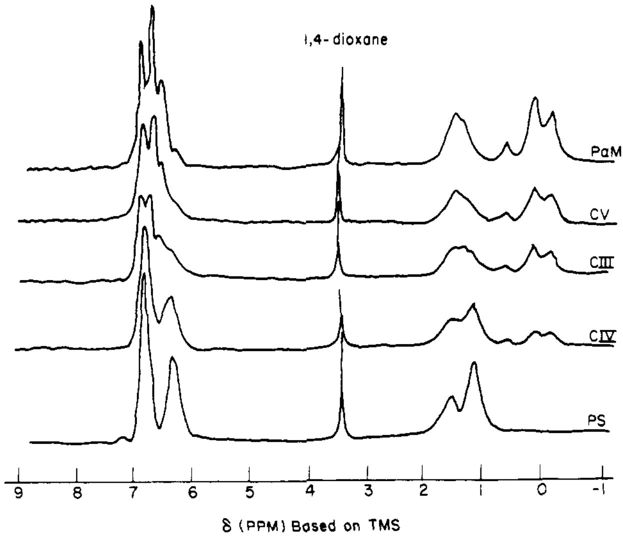

Figure 3. Traces of the NMR spectrum for the homopolymers, PS and PαMS, and PαMS-PS diblock copolymers synthesized in this study (see Table I for block molecular weights).

Measurement of Glass Transition Temperature. The glass transition temperature (T_g) for each of the PαMS-PS block copolymers synthesized was measured using a Perkin-Elmer DSC 7 Series unit. Prior to measurement, the baseline was obtained using two empty aluminum pans, which was later used for baseline correction. The DSC samples were prepared by compression molding at room temperature. Conditions used for typical DSC runs were to first heat the sample to 230 °C at a rate of 10 °C/min and then anneal it for 2 min, and subsequently to quench the sample to 35 °C at a rate of 200 °C/min. During each run nitrogen gas was directed into the DSC cell in order to minimize degradation of the sample. This cycle was repeated several times. Reproducibility of the value of T_g was found to be accurate to within ±1.5 °C. The values of T_g were read off from DSC thermograms at the midpoint of change in the heat flow (milliwatts), which was normalized to W/g using the measured weight of sample.

Figure 4 gives traces of DSC thermograms for the PS and PαMS homopolymers, and PαMS-PS diblock copolymers synthesized for this study. It can be seen in Figure 4 that each block copolymer sample has a single value of T_g, indicating homogeneity of the block copolymers, and that the value of T_g of the block copolymer increases monotonically as the weight fraction of the PαMS block increases. In reference to Figure 4, the range of the transition is indicated by two arrows, one pointing upward on the left side to indicate the onset of transition (T_{gi}) and the other pointing downward on the right side to indicate the completion of transition (T_{gf}). Notice in Figure 4 that values of $\Delta T = T_{gf} - T_{gi}$ for the block copolymers are much larger than those of the constituent components. Table II gives a summary of T_g based on the midpoint in the transition and ΔT for the seven PαMS-PS block copolymers and constituent homopolymers synthesized for this study, showing that samples BII and CII, having almost equal lengths of PαMS and PS blocks, have the largest values of ΔT. Earlier, other research groups[2,3] also reported similar observations for PαMS-PS diblock copolymers, as well as for PαMS-PS-PαMS and PS-PαMS-PS triblock copolymers. It is of interest to mention that several research groups[10–13] investigated the glass transition behavior of blends of homopolymers PαMS and PS and reported a very broad range for the glass transition in a blend having almost equal amounts of the constituent components. Of particular note is a recent study by Schneider and co-workers,[14] who observed a broad range of glass transition occurring in blends of polystyrene (PS) and poly(vinyl methyl ether) (PVME); for instance, the value of ΔT for the 50/50 PS/PVME mixture spanned over 60 °C. They attributed the existence of such a broad range of T_g for certain blend compositions in PS/PVME mixtures to local composition fluctuations of microdomains.

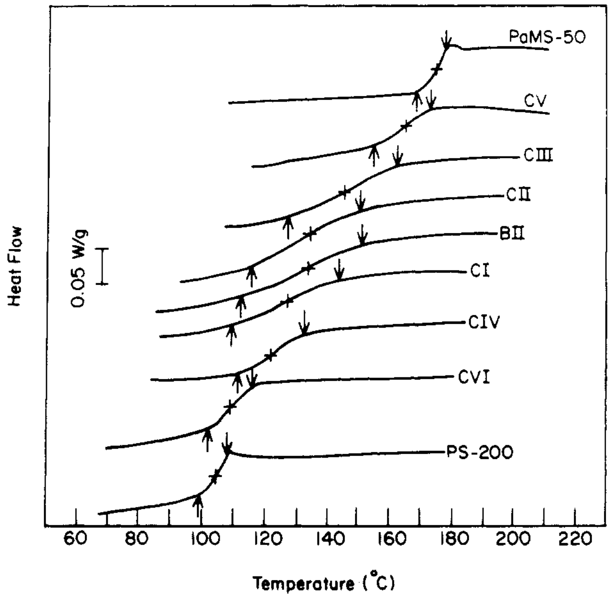

Figure 4. Traces of the DSC thermogram for the homopolymers, PS and PαMS, and seven PαMS-PS diblock copolymers synthesized in this study (see Table I for the block molecular weights of each sample). Heating rate employed was 10 °C/min. On each curve, the arrow pointing upward on the left side denotes the temperature (T_{gi}) at which the transition begins and the arrow pointing downward on the right side denotes the temperature (T_{gf}) at which the transition ends.

Table II
Summary of the Glass Transition Temperatures for the PαMS-PS Block Copolymers Synthesized

sample code	T_g, °C[a]	$T_{gf} - T_{gi}$, °C
PS-200	104	9
CVI	109	12
CIV	122	21
CI	127	35
BII	134	39
CII	135	37
CIII	145	35
CV	164	19
PαMS-50	175	9

[a] Based on the midpoint in the transition.

It should be pointed out that the smallest size that can be detected by DSC is about 20 nm, which may not be small enough to describe the motion of the PS or PαMS block in a very small region around the block copolymer. We speculate here that the PαMS or PS block can move around with its own mobility, and not with the average mobility of the block copolymer. Thus, we propose further that the onset point (i.e., T_{gi}) in the transition observed in Figure 4 represents the motion of the PS block which has greater mobility than the PαMS block, and not the average motion of the block copolymer itself. Such hypothesis can be proved or disproved by using a more sophisticated analytical technique (e.g., solid-state NMR) than DSC.

The dependence of glass transition temperature T_g of PαMS-PS diblock copolymers on block composition determined in this study is summarized in Figure 5, in which the circle represents the midpoint in the transition, the triangle represents the initial point (T_{gi}) in the transition, and the square represents the final point (T_{gf}) in the transition. In order to facilitate our discussion, we have drawn four curves in Figure 5; namely, curve 1 represents prediction with the linear relationship, $T_g = w_{\mathrm{P\alpha MS}} T_{g,\mathrm{P\alpha MS}} + w_{\mathrm{PS}} T_{g,\mathrm{PS}}$, and curve 2 represents prediction with the Fox equation[15]

$$1/T_g = w_{\mathrm{P\alpha MS}}/T_{g,\mathrm{P\alpha MS}} + w_{\mathrm{PS}}/T_{g,\mathrm{PS}} \qquad (4)$$

curve 3 is drawn through the data points representing T_{gi}, and curve 4 is drawn through the data points representing T_{gf}. Note in eq 4 that $w_{\mathrm{P\alpha MS}}$ and w_{PS} are the weight fractions of PαMS and PS blocks, respectively, in the block copolymer, and $T_{g,\mathrm{P\alpha MS}}$ and $T_{g,\mathrm{PS}}$ are the glass transition temperatures of PαMS and PS blocks, respectively. In drawing curves 1 and 2 given in Figure 5, we used $T_{g,\mathrm{P\alpha MS}} = 175$ °C and $T_{g,\mathrm{PS}} = 104$ °C, as determined in this study. These values are slightly higher than those reported in the literature[16-18] ($T_{g,\mathrm{P\alpha MS}} = 172$ °C and $T_{g,\mathrm{PS}} = 100$ °C), but a recent study by Widmaier and Mignard[12] reports the value of $T_{g,\mathrm{P\alpha MS}} = 175$–$177$ °C for molecular weights ranging from 6.4×10^4 to 3.65×10^5. It can be seen in Figure 5 that the measured values of T_g based on the midpoint in the transition (circle) are in good agreement with prediction by the Fox equation. We also observe in Figure 5 that the linear relationship works equally well. Earlier, Phalip et al.[19] reported the results of T_g measurements for PαMS-PS diblock copolymers, which are very similar to ours, given in Figure 5. It should be mentioned that, very recently, Suzuki and Miyamoto[20] made a theoretical prediction that the glass transition temperatures of compatible block copolymers would follow the linear relationship. Such prediction seems to have validity if we choose the midpoint in the transition as the T_g of the PαMS-PS diblock copolymers investigated in the present study. It is worth pointing out, however, that in Figure 5 we observe *negative* deviations from linearity when using the initial point in the transition (T_{gi}) and *positive* deviations from linearity when using the final point in the transition (T_{gf}).

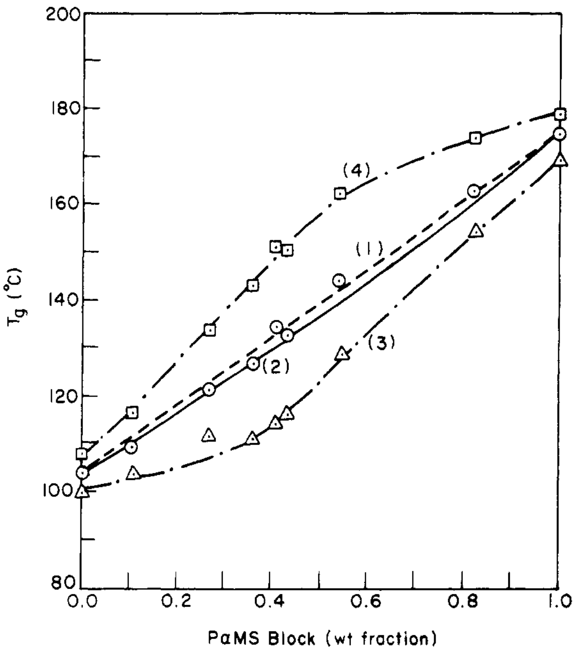

Figure 5. Plots of glass transition temperature (T_g) versus weight fraction of PαMS in the PαMS-PS diblock copolymers synthesized in this study, in which ⊙ represents the midpoint in the transition, ▲ represents the initial point (T_{gi}) in the transition, and ◻ represents the final point (T_{gf}) in the transition. Here curve 1 describes the prediction based on a linear relationship, curve 2 describes the prediction based on Fox's equation, curve 3 is drawn through the data points of T_{gi}, and curve 4 is drawn through the data points of T_{gf}.

Measurement of Dynamic Viscoelastic Properties. Samples were prepared for oscillatory shear flow measurements by first dissolving a predetermined amount of PαMS-PS block copolymer in benzene (5 wt % solid in solution) in the presence of an antioxidant (Irganox 1010, Ciba-Geigy Group). The solution was freeze-dried at room temperature for 3 days under vacuum and dried at 110 °C for 2 days also under vacuum. The dried sample was compression-molded at 180 °C for the seven PαMS-PS block copolymers and homopolymer PS synthesized and at 200 °C for homopolymer PαMS into a sheet of about 1 mm in thickness. Finally, the samples were annealed for 3 h at a temperature about 20 °C above the T_g of the block copolymer. A Rheometrics mechanical spectrometer (RMS) in the parallel-plate mode (8-mm-diameter plates) was used to measure the dynamic storage modulus $G'(\omega)$ and dynamic loss modulus $G''(\omega)$, as functions of angular frequency (ω) at various temperatures, for each of the block copolymer samples. The temperature control was satisfactory to within ±1 °C. In the oscillatory measurements a very low strain was used, which was well within the linear viscoelastic range of the materials investigated. All experiments were conducted in the presence of nitrogen in order to preclude oxidative degradation of the samples.

Experimental Results and Discussion

Factors Affecting the Degradation of Homopolymer PαMS and PαMS-PS Diblock Copolymer. It has been reported[4,17,21,22] that PαMS is susceptible to degradation when it is held at an elevated temperature for a certain period. This subject was very important to us because the main thrust of the present study was to undertake rheological measurements of both homopolymer PαMS and PαMS-PS diblock copolymers at elevated temperatures (above 170 °C). Therefore, before initiating any rheological measurement, we had to investigate the conditions under which the degradation of homopolymer PαMS and PαMS-PS diblock copolymer might take place.

In this study, using thermogravimetric analysis (TGA) (Du Pont, Model 951) we measured the weight loss of homopolymer PαMS and PαMS-PS diblock copolymers that we had synthesized, at a fixed temperature as a function of time. Specifically, we monitored the weight loss, if any, of the sample under an environment of air and nitrogen, respectively, and with and without an antioxidant in the sample. In preparing samples for TGA measurements, a predetermined amount (5 wt %) of polymer (PαMS or PαMS-PS diblock copolymer) was dissolved in benzene with different amounts (0.2 and 0.5 wt %) of an antioxidant (Irganox 1010, Ciba-Giegy Group). The solution was freeze-dried at room temperature for 3 days and dried further at 100 °C for 2 days under vacuum. After the polymer was dried completely, specimens were prepared in the form of a compact cake (ca. 15–20 mg) by compression molding at room temperature.

Figure 6 gives traces of the TGA thermogram for PαMS-100 with and without an antioxidant at 230 and 240 °C, respectively, for 60 min by having an air flow of 60 cm^3/min over the specimen. It can be seen in Figure 6 that at 230 °C the sample without the antioxidant had a weight loss of 42% at the end of 60 min, while the sample with 0.2 wt % Irganox had no discernible weight loss; at 240 °C the sample without the antioxidant had a weight loss of 67%, while the sample with 0.2 wt % Irganox began to lose weight after 37 min and had a weight loss of 5.3% at the end of 60 min; and the sample with 0.5 wt % Irganox had no discernible weight loss at the end of 60 min. These observations indicate to us that the presence and amount of an antioxidant in PαMS-100 play an important role in determining the extent of degradation of the sample for a fixed period.

Figure 7 gives traces of the TGA thermogram for PαMS-100 with and without an antioxidant, under the flow of nitrogen. The following observations are worth noting on Figure 7: (a) at 230 °C, the specimen without an antioxidant has *no* discernible weight loss for 60 min; (b) at 240 °C, the specimen without an antioxidant starts to degrade after 53 min and the total weight loss at the end of 60 min is negligibly small, whereas the specimen with an antioxidant has no discernible weight loss at the end of 60 min; (c) at 250 °C, the sample without an antioxidant starts to degrade after 18 min and the total weight loss at the end of 60 min is 0.8%, and the sample with 0.5 wt % Irganox starts to degrade after 25 min and the total weight loss at the end of 60 min is 0.7%. The above observations indicate to us that the exclusion of oxygen in the environment under which the TGA measurements were taken has reduced considerably the extent of degradation in the PαMS-100 specimen for a fixed period.

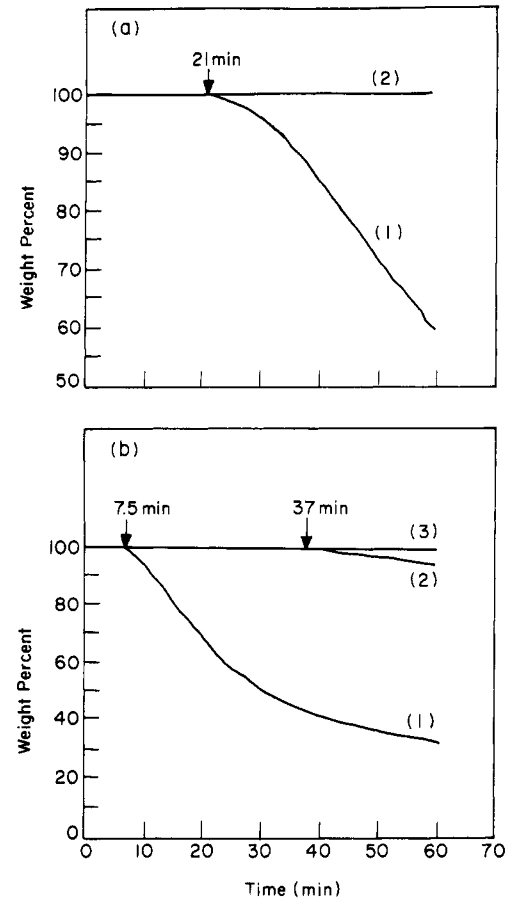

Figure 6. Traces of the TGA thermogram for PαMS-100 obtained under an environment of air: (a) curve 1 for a sample without an antioxidant at 230 °C, and curve 2 for a sample with 0.2 wt % Irganox at 230 °C; (b) curve 1 for a sample without an antioxidant at 240 °C, curve 2 for a sample with 0.2 wt % Irganox at 240 °C, and curve 3 for a sample with 0.5 wt % Irganox at 240 °C.

Figure 8 gives traces of the TGA thermogram for sample CV, which has about 80 wt % PαMS in PαMS-PS diblock copolymer (see Table I), with and without an antioxidant under the flow of air and nitrogen, respectively. It is quite clear from Figure 8 that there is *no* discernible weight loss in the specimen under the flow of nitrogen at temperatures up to 260 °C when it contains 0.5 wt % Irganox. This has led us to conduct all rheological measurements, presented below, by adding 0.5 wt % Irganox to all samples (i.e., both homopolymer and PαMS-PS diblock copolymers) and under the atmosphere of nitrogen in the specimen test chamber.

In order to investigate a change in molecular weight, if any, after each specimen was prepared by compression molding and, also, after rheological measurements, using GPC we measured the molecular weights of the specimens. Figure 9 gives traces of the GPC chromatogram for PαMS-100 with 0.5 wt % Irganox, in which samples had the following histories: (a) as synthesized, (b) after compression molding at 200 °C, (c) after oscillatory shear measurement at 230 °C, and (d) after oscillatory shear measurement at 240 °C. Note that each run of oscillatory shear measurement lasted about 20 min. It can be seen in Figure 9 that the peak positions remain almost the same after being subjected to oscillatory shear flow at 240 °C under a nitrogen atmosphere. This observation was corroborated our independent TGA measurements, presented above, that there would be a negligible amount, if any, of degradation in the samples during our rheological measurements presented below.

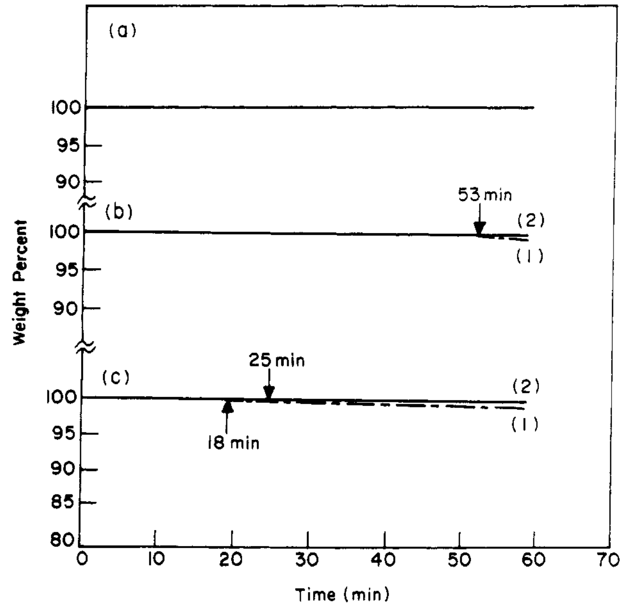

Figure 7. Traces of the TGA thermogram for PαMS-100 obtained under an environment of nitrogen: (a) sample without an antioxidant at 230 °C; (b) curve 1 for a sample without an antioxidant at 240 °C, and curve 2 for a sample with 0.5 wt % Irganox at 240 °C; (c) curve 1 for a sample without an antioxidant at 250 °C, and curve 2 for a sample with 0.5 wt % Irganox at 250 °C.

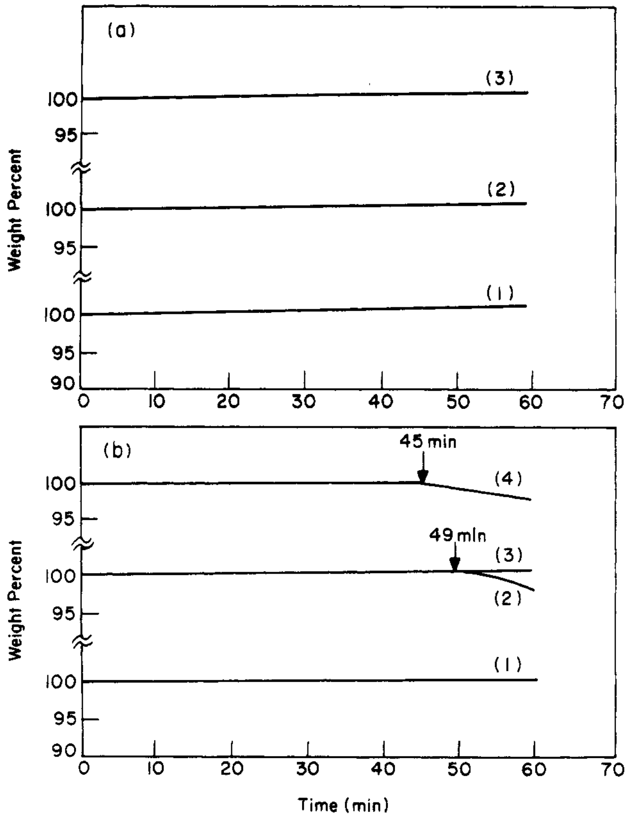

Figure 8. Traces of the TGA thermogram for a PαMS-PS diblock copolymer, sample CV: (a) (under an environment of nitrogen) curve 1 for a sample with 0.5 wt % Irganox at 240 °C, curve 2 for a sample with 0.5 wt % Irganox at 250 °C, and curve 3 for a sample with 0.5 wt % Irganox at 260 °C; (b) (under an environment of air) curve 1 for a sample without an antioxidant at 230 °C, curve 2 for a sample without an antioxidant at 240 °C, and curve 3 for a sample with 0.5 wt % Irganox at 240 °C, and curve 4 for a sample with 0.5 wt % Irganox at 250 °C.

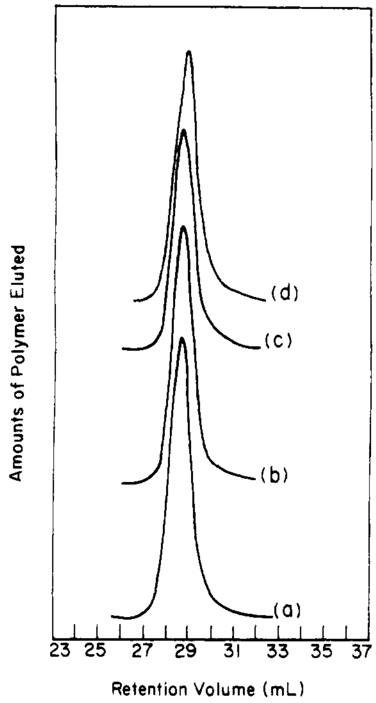

Figure 9. Traces of the GPC chromatogram for PαMS-100: (a) sample as synthesized, (b) sample after compression molding at 200 °C for 20 min, (c) sample after oscillatory shear flow experiment at 230 °C for 20 min, and (d) sample after oscillatory shear flow experiment at 240 °C for 20 min.

Earlier, some research groups[4,17,21,22] reported the degradation of PαMS at elevated temperatures, whereas other research groups[3,16] reported that no discernible degradation of PαMS was observed when experiments were carried out under a nitrogen atmosphere. Specifically, Cowie and Bywater[21] reported weight losses of 5 and 10.5% at 226 and 236 °C, respectively, when the experiments were carried out under vacuum for 1 h. They noted further that degradation occurred in the PαMS samples that were prepared either with monofunctional or difunctional initiators. Hansen and Shen[4] reported a decrease of about 30% in molecular weight after homopolymer PαMS and PαMS-PS-PαMS and PS-PαMS-PS triblock copolymer samples, respectively, were subject to compression molding and dynamic mechanical testing. Odani et al.[17] reported a decrease of about 20% in molecular weight after a PαMS specimen had been subjected to dynamic mechanical testing at 230 °C for about 30 min. Such large drops in molecular weight could have been avoided if an antioxidant had been used.

Homogeneity of the PαMS-PS Diblock Copolymers Synthesized. It is a well-established fact today that, in general, block copolymers form microdomains at temperatures below a certain critical value, often referred to as the order–disorder transition temperature (T_r) (or microphase-separation transition temperature). Three factors, namely, (a) block length ratio, (b) the total molecular weight, and (c) the extent of thermodynamic compatibility (i.e., the interaction parameter) between the constituent blocks, determine the formation of microdomains.[23] By applying the "confined chain" theory to a polystyrene-*block*-polyisoprene (SI) copolymer, Meier[24] has concluded that a microdomain structure can form when the molecular weight of the polystyrene block becomes about 5000 or larger. On the other hand, due to very good thermodynamic compatibility between polystyrene and poly(α-methylstyrene), it is reported in the literature[1-3] that *no* microdomain structure may be formed in PS-PαMS, PS-PαMS-PS, or PαMS-PS-PαMS block copolymers even when the molecular weights of the constituent blocks

Table III
Predicted Order–Disorder Transition Temperatures (T_r) for PαMS-PS, PαMS-PS-PαMS, and PS-PαMS-PS Block Copolymers

sample code	block molecular weight (× 10^{-3})	predicted T_r, °C	measured T_g, °C	ref
	a. PαMS-PS Diblock Copolymers			
BP-I	52.5PαMS-37.4PS	−164	134	1
BP-IIA	79.8PαMS-70.2PS	−77	132	1
BP-III	223.4PαMS-196.6PS	173	130	1
D1	274.6PαMS-254.4PS	244	101; 170	2
D2	548.8PαMS-431.2PS	420	130; 170	2
D3	259.2PαMS-460.8PS	291	103	2
DB1	132.6PαMS-127.4PS	41	118 to 125	3
DB2	358.4PαMS-281.6PS	298	101; 170	3
DB4	614.8PαMS-445.2PS	438	103; 170	3
BII	52PαMS-70PS	−122	134	this study
CI	54PαMS-94PS	−102	127	this study
CII	99PαMS-145PS	9	135	this study
CIII	135PαMS-120PS	9	145	this study
CIV	50PαMS-130PS	−102	122	this study
CV	122PαMS-26PS	−176	164	this study
CVI	21PαMS-167PS	−202	109	this study
	b. PαMS-PS-PαMS Triblock Copolymer			
TB8	116.4PαMS-737.2PS-116.4PαMS	86	111	3
TB9	185.6PαMS-788.8PS-185.6PαMS	223	112; 188	3
F	22.1PαMS-119.7PS-22.1PαMS	−192	159	4
G	27PαMS-66PS-27PαMS	−181	173	4
	c. PS-PαMS-PS Triblock Copolymer			
TB1	304.8PS-660.4PαMS-304.8PS	347	112; 180	3
TB2	406.7PS-846.6PαMS-406.7PS	424	113; 180	3
A	72.7PS-7.6PαMS-72.7PS	−256	140	4
B	50.1PS-20.9PαMS-50.1PS	−221	140	4
C	42.6PS-43.9PαMS-42.6PS	−179	150	4
D	42.9PS-62.1PαMS-42.9PS	−156	158	4
E	16.3PS-60.4PαMS-16.3PS	−211	169	4

become as large as about 2×10^5. Such observations were based on the findings of a single glass transition temperature, as determined by either DSC or dynamic mechanical measurements.

So far, no theoretical predictions have been reported in the literature on the range of block molecular weights that give rise to homogeneous PαMS-PS, PαMS-PS-PαMS, or PS-PαMS-PS block copolymers. In this study, using the currently held theories due to Helfand and Wasserman[25] and Leibler,[23] we calculated values of T_r for the seven PαMS-PS block copolymers that we have synthesized, as well as for those PαMS-PS diblock and PαMS-PS-PαMS and PS-PαMS-PS triblock copolymers reported in the literature.[1-4] The stipulation made was that the formation of microdomains in any of these block copolymers would not be possible if predicted values of T_r are lower than about 170 °C, which is the T_g of PαMS. We have found that predicted values of T_r from Leibler's theory were unrealistically high, about 140 °C higher than those predicted by Helfand–Wasserman's theory, and therefore a summary of predicted values of T_r only from Helfand–Wasserman's theory is given in Table III, together with information on T_g's determined experimentally.

In the calculations of the T_r given in Table III we have used the following expression for the interaction energy density Λ:[26]

$$\Lambda = 0.0608 + 0.0018\phi_1 - 0.56 \times 10^{-4}T \tag{5}$$

where ϕ_1 is the volume fraction of PαMS in the PαMS/PS pair, T is the absolute temperature, and Λ is expressed in calories per centimeter cubed. And we used the following expression for the specific volumes:

$$v_{\mathrm{PS}} = 0.9199 + 5.098 \times 10^{-4}(T - 273) + 2.354 \times 10^{-7}(T - 273)^2 + [32.46 + 0.1017(T - 273)]/M_{\mathrm{w,PS}} \tag{6}$$

for polystyrene[27] in which $M_{\mathrm{w,PS}}$ is the molecular weight of polystyrene and

$$v_{\mathrm{P\alpha MS}} = 0.87 + 5.08 \times 10^{-4}(T - 273) \tag{7}$$

for poly(α-methylstyrene).[28] Note in eqs 6 and 7 that v_{PS} and $v_{\mathrm{P\alpha MS}}$ are expressed in centimeter cubed per gram and T is the absolute temperature.

It is very encouraging to observe in Table III that, except for two cases (samples BP-III and D3), whenever a single value of T_g was observed experimentally the predicted values of T_r are *below* 170 °C, suggesting that these block copolymers are in the homogeneous state. The predicted value of T_r (173 °C) for sample BP-III lies on the boundary between the homogeneous and microphase-separated states, depending on to whose data one refers. It should be mentioned that precise determination of T_g varies with the type of instrument employed, as well as the purity of the samples to a certain extent. According to our experience with block copolymers of styrene and isoprene, and block copolymers of styrene and butadiene, Helfand–Wasserman's theory predicts values of T_r to within ±20 °C when compared with experiment. Therefore, we can regard the predicted values of T_r for sample BP-III as being very reasonable. However, we cannot explain why DSC measurements of sample D3 showed a single value of T_g, whereas the predicted value of T_r is about 120 °C above the T_g of PαMS.

Dynamic Viscoelastic Properties of PαMS-PS Diblock Copolymers. Frequency–temperature superposition has been extensively used to obtain temperature-independent master curves for flexible homopolymers by shifting values of dynamic storage and loss moduli, $G'(\omega)$ and $G''(\omega)$, along the frequency ω axis.[18] In such an attempt, one chooses a particular temperature as a reference temperature and shifts the values of G' and G'' obtained at all other temperatures to the corresponding values at the reference temperature. It turns out that shift factor a_T, which is a function of temperature, enables

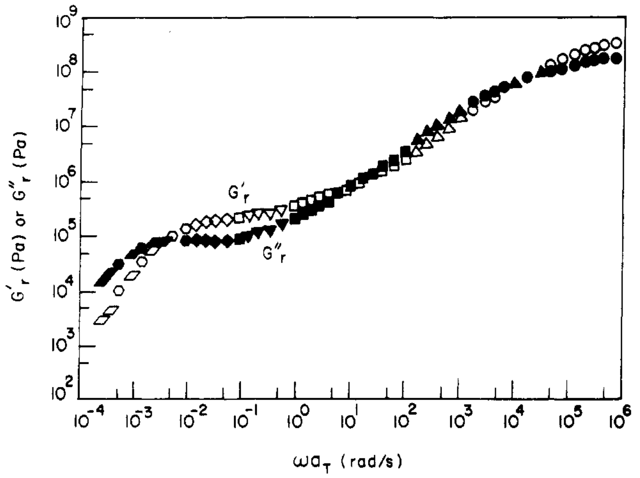

Figure 10. Logarithmic plots of G'_r and G''_r versus ωa_T for sample CIV with 154 °C as a reference temperature: (○, ●) 127 °C; (△, ▲) 135 °C; (□, ■) 154 °C; (▽, ▼) 175 °C; (◇, ◆) 194 °C; (⬡, ⬢) 214 °C; (▱, ▰) 234 °C.

one to obtain master curves.

Figure 10 gives logarithmic plots of reduced storage modulus G'_r and reduced loss modulus G''_r versus ωa_T for sample CIV, where G'_r and G''_r are defined by $G'T_0\rho_0/T\rho$ and $G''T_0\rho_0/T\rho$, respectively, T_0 is the reference temperature which in the present case is taken as 154 °C, and ρ_0 and ρ are the densities at temperatures T_0 and T, respectively. In obtaining Figure 10, values of a_T were determined from the following expression:

$$a_T = \frac{\eta_0(T)\rho(T_0)T_0}{\eta_0(T_0)\rho(T)T} \tag{8}$$

which is denoted by a circle in Figure 11. Also given in Figure 11 is the prediction (solid curve) made by the WLF equation:

$$\log a_T = \frac{-13.7(T - T_g)}{50 + T - T_g} \tag{9}$$

where T_g is taken as 122 °C (see Table II).

It should be mentioned that the dynamic moduli given in Figure 10 were measured at seven different temperatures ranging from 127 to 234 °C and the values of ωa_T span over 10 decades. Notice in Figure 10 that G'_r initially increases with increasing ωa_T and then tends to level off, and finally increases again with increasing ωa_T, while G''_r initially increases with increasing ωa_T and then goes through a minimum, and finally increases again with increasing ωa_T. Earlier, Colby et al.[29] reported similar behavior for a flexible monodisperse polybutadiene. What is of great interest in Figure 10 is that when applying frequency–temperature superposition, the PαMS-PS diblock copolymer, sample CIV, exhibits temperature-independent correlations, very similar to flexible homopolymers. Previously, Han and Kim[30] pointed out that microphase-separated block copolymers do not follow temperature–frequency superposition. Therefore one can conclude from Figure 10 that sample CIV is homogeneous.

Notice in Figure 10 that a distinct plateau value for G'_r for sample CIV is not discernible. Therefore, we followed the suggestion of Kraus and Rollmann[31] that, in such an instance, the plateau modulus $G°_N$ may be determined by the value of G' at which loss tangent (tan δ) goes through a minimum. Figure 12 gives plots of tan δ versus ωa_T for sample CIV, which were obtained at nine different temperatures. From Figure 12 we estimate the value of $G°_N$ for sample CIV to be about 2.45 × 10^5 Pa.

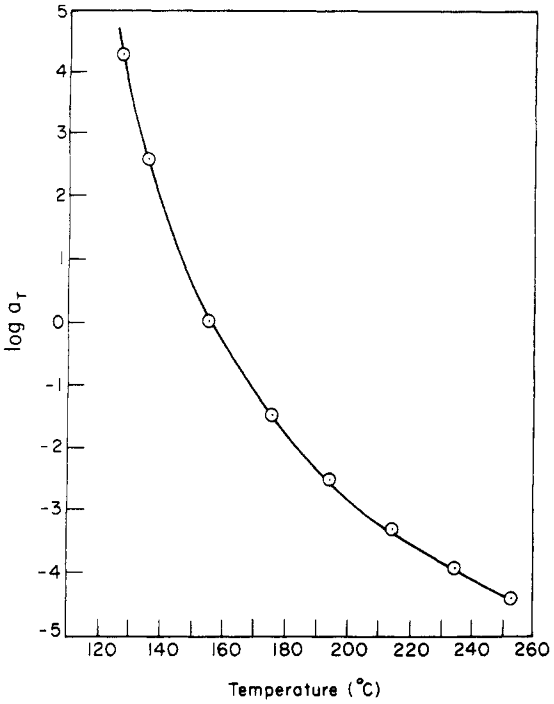

Figure 11. Plots of log a_T versus temperature for sample CIV, where solid curve describes the prediction with the WLF equation using T_g = 122 °C.

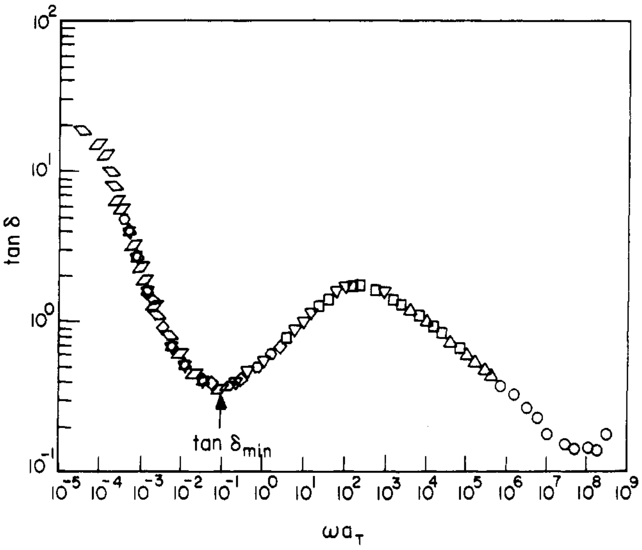

Figure 12. Logarithmic plots of tan δ versus ωa_T for sample CIV with 154 °C as a reference temperature: (○) 115 °C; (△) 127 °C; (□) 135 °C; (▽) 154 °C; (◇) 175 °C; (⬡) 194 °C; (▱) 214 °C); (✡) 234 °C; (▭) 253 °C.

Figure 13 gives plots of G', G'', and tan δ versus temperature for sample CIV, which were obtained by increasing the temperature stepwise, 3 °C in each step, at a fixed angular frequency of 10 rad/s. Since a plateau value for G' is not discernible in Figure 13, as was done above in reference to Figure 12, we estimate the value of $G°_N$ for sample CIV to be about 2.51 × 10^5 Pa from the value of G' at which tan δ goes through a minimum. It is of interest to observe that two different types of experiments, frequency sweep and temperature sweep, respectively, give rise to essentially the same value of $G°_N$ for the block copolymer, sample CIV. Observe further in Figure 13 that the temperature at which tan δ goes through a maximum is about 142 °C, which can be regarded as the T_g of sample CIV. Notice that the value of T_g determined from Figure 13 (i.e., from dynamic viscoelastic measurement) is about

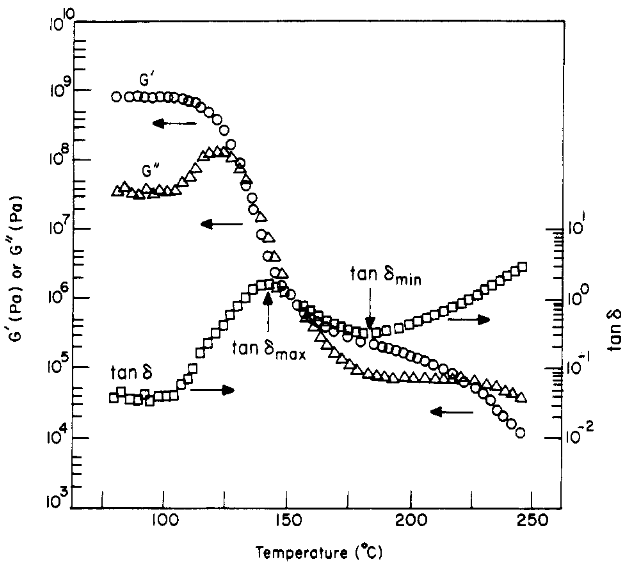

Figure 13. Plots of log G', log G'', and log tan δ versus temperature for sample CIV at a fixed angular frequency of 10 rad/s. The temperature sweep experiment was conducted at the heating rate of 3 °C per step. The value of G' at tan δ_{min} is 2.51×10^5 Pa, and the value of T_g at tan δ_{max} is 142 °C.

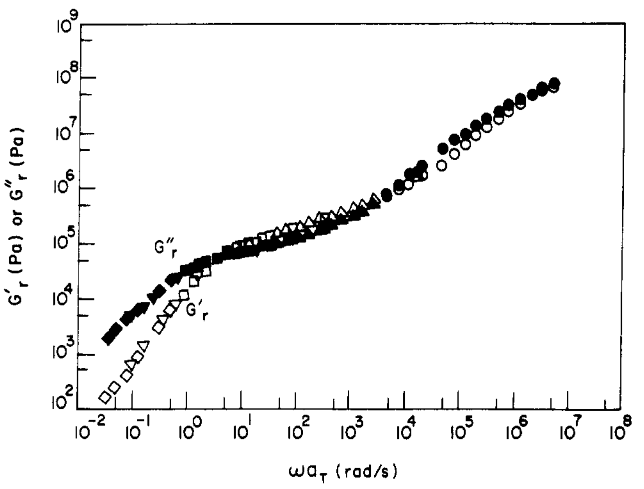

Figure 14. Logarithmic plots of G'_r and G''_r versus ωa_T for sample BII with 211 °C as a reference temperature: (○, ●) 151 °C; (△, ▲) 171 °C; (□, ■) 191 °C; (▽, ▼) 211 °C; (◇, ◆) 231 °C.

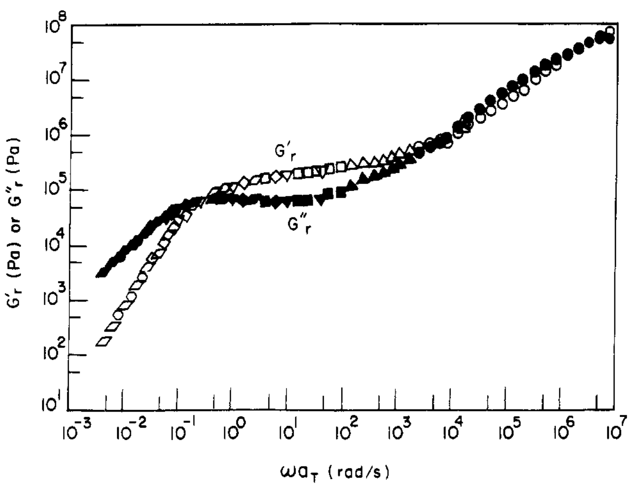

Figure 15. Logarithmic plots of G'_r and G''_r versus ωa_T for sample CII with 210 °C as a reference temperature: (○, ●) 151 °C; (△, ▲) 171 °C; (□, ■) 191 °C; (▽, ▼) 210 °C; (◇, ◆) 230 °C; (○, ●) 241 °C; (▱, ▰) 251 °C.

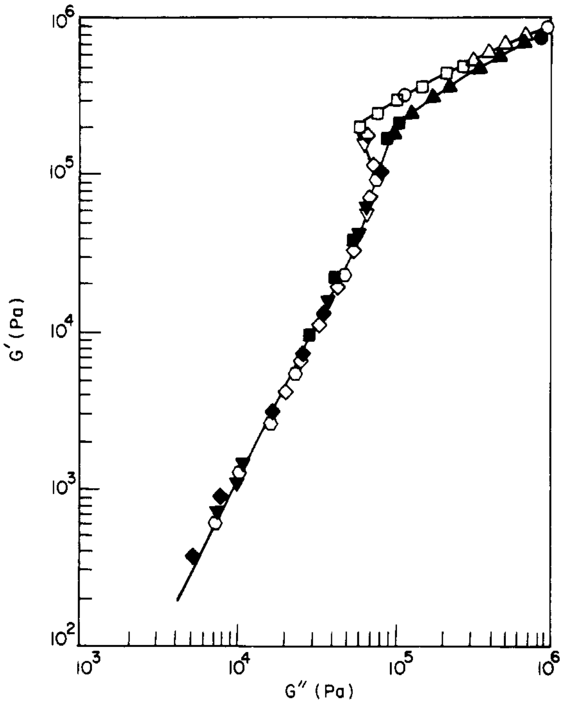

Figure 16. Logarithmic plots of G' versus G'' for (a) sample BII at various temperatures (°C), (●) 151; (▲) 171; (■) 191; (▼) 211; (◆) 231; and (b) sample CII at different temperatures (°C), (○) 151; (△) 171; (□) 191; (▽) 210; (◇) 230; (○) 241.

20 °C higher than that (122 °C) determined from DSC measurement (see Table II). It is a well-established fact today that the values of T_g determined from dynamic viscoelastic measurements depend on the angular frequencies used.

Figure 14 gives logarithmic plots of G'_r and G''_r versus ωa_T for sample BII, which were obtained at temperatures ranging from 151 to 231 °C. Similar plots are given in Figure 15 for sample CII, which were obtained at temperatures ranging from 151 to 251 °C. Notice in Table I that these two block copolymer samples have almost the same weight fraction of PαMS, but a very large difference in total molecular weight, and that the molecular weights of PαMS and PS blocks in the two block copolymers are larger than the entanglement molecular weights. However, when values of G' are plotted against values of G'' on logarithmic coordinates, as displayed in Figure 16, we observe that the two block copolymers give rise to a correlation, which becomes not only independent of temperature, but also independent of molecular weight in the terminal region. Such an observation has been reported for entangled, flexible homopolymers by Han and co-workers,[32-35] and Han and Jhon[34] offered a molecular interpretation of the experimental observation.

Recently, Han and co-workers[30,36-39] have reported that log G' versus log G'' plots depend on temperature for microphase-separated block copolymers, but become independent of temperature when the block copolymers become *homogeneous* as the temperature is raised above a certain critical value, i.e., order–disorder transition temperature. In light of the previous studies of Han and co-workers, we can conclude from Figure 16 that block copolymer samples BII and CII are *homogeneous* in the range of temperatures where the rheological measurements were taken.

Figure 17 gives logarithmic plots of G'_r and G''_r versus ωa_T for sample CVI, which were obtained at temperatures ranging from 116 to 236 °C. It can be seen in Figure 17 that temperature–frequency superposition gives rise to a

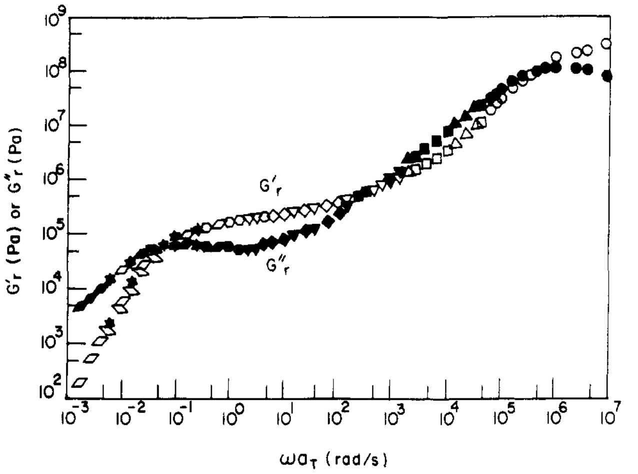

Figure 17. Logarithmic plots of G'_r and G''_r versus ωa_T for sample CVI with 162 °C as a reference temperature: (○, ●) 116 °C; (△, ▲) 126 °C; (□, ■) 131 °C; (▽, ▼) 142 °C; (◇, ◆) 162 °C; (○, ●) 181 °C; (▱, ▰) 200 °C; (☼, ✱) 220 ° C; (⊂, ▬) 239 °C.

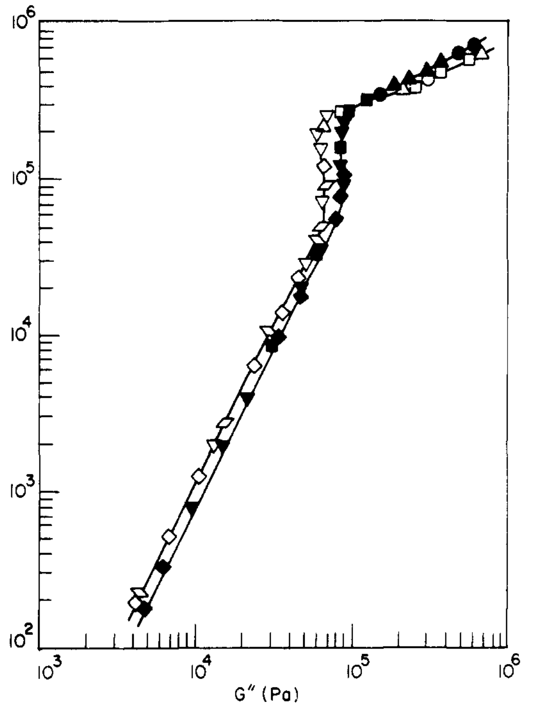

Figure 18. Logarithmic plots of G' versus G'' for (a) sample CIV at various temperatures (°C), (●) 155; (▲) 175; (■) 194; (▼) 214; (◆) 234; and (b) sample CVI at various temperatures (°C), (○) 131; (△) 142; (□) 162; (▽) 181; (◇) 200; (▱) 220; (⊂) 239.

temperature-independent correlation for sample CVI, indicating that this block copolymer is homogeneous. Figure 18 gives plots of log G' versus log G'' for samples CIV and CVI at various temperatures, showing that each block copolymer sample lies on a single curve, independent of temperature, but that the two samples do *not* lie on the same curve. Note in Table I that these two block copolymers have almost the same total molecular weight (ca. 1.8×10^5) but different block length ratios. The results displayed in Figure 18 suggest to us that the elasticity of the block copolymer varies with block length ratio, which is very reasonable.

Logarithmic plots of G'_r and G''_r versus ωa_T are given in Figure 19 for sample CI at temperatures ranging from 136 to 240 °C, in Figure 20 for sample CIII at temperatures ranging from 161 to 236 °C, and in Figure 21 for sample CV at temperatures ranging from 172 to 241 °C.

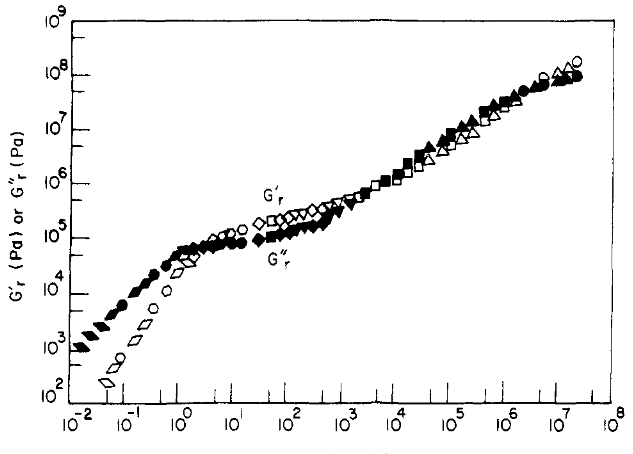

Figure 19. Logarithmic plots of G'_r and G''_r versus ωa_T for sample CI with 210 °C as a reference temperature: (○, ●) 136 °C; (△, ▲) 146 °C; (□, ■) 154 °C; (▽, ▼) 173 °C; (◇, ◆) 192 °C; (○, ●) 210 °C; (▱, ▰) 220 °C; (⊂, ▬) 240 °C.

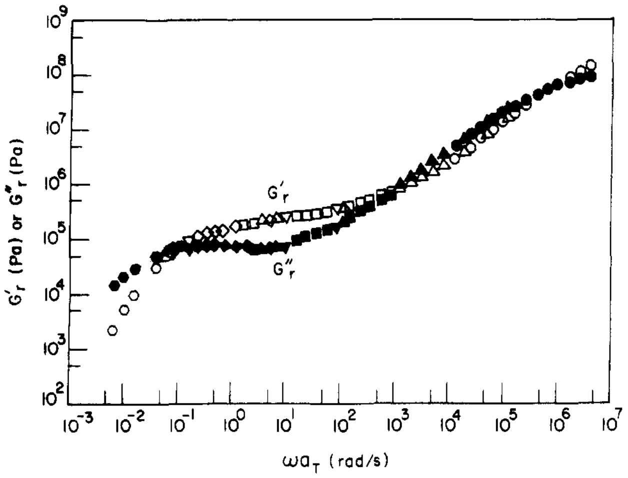

Figure 20. Logarithmic plots of G'_r and G''_r versus ωa_T for sample CIII with 211 °C as a reference temperature: (○, ●) 161 °C; (△, ▲) 171 °C; (□, ■) 191 °C; (▽, ▼) 211 °C; (◇, ◆) 226 °C; (○, ●) 236 °C.

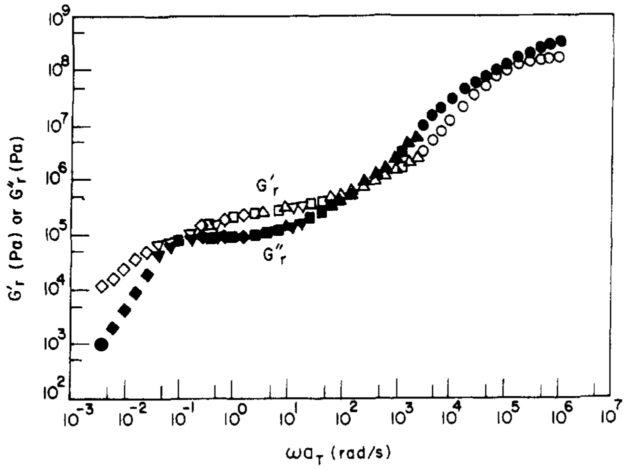

Figure 21. Logarithmic plots of G'_r and G''_r versus ωa_T for sample CV with 212 °C as a reference temperature: (○, ●) 172 °C; (△, ▲) 192 °C; (□, ■) 212 °C; (▽, ▼) 226 °C; (◇, ◆) 241 °C.

We can conclude from Figures 19–21 that all three block copolymers, samples CI, CIII, and CV, are homogeneous. Owing to the limited space available here, we do not show plots of log G' versus log G'' for the three block copolymers, which also exhibit temperature-independent correlations.

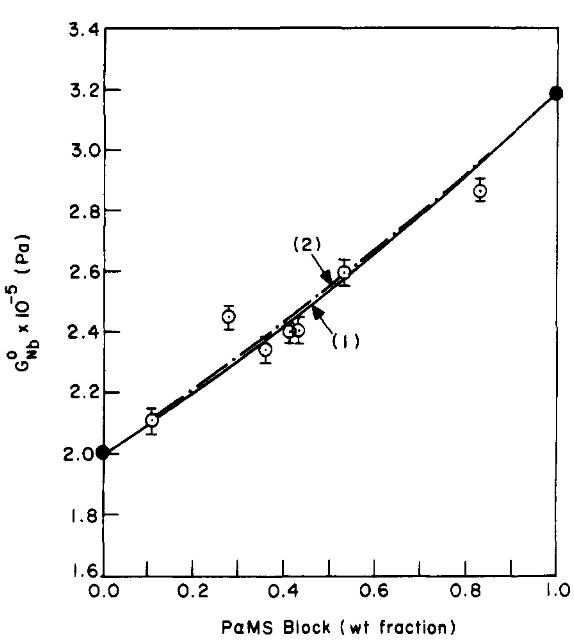

Figure 22. Plots of plateau modulus $G°_{Nb}$ versus weight fraction of PαMS in PαMS-PS diblock copolymers, where curve 1 describes the prediction made with the 3.4-power blending law, and curve 2 describes the prediction made with the quadratic blending law.

It can be concluded from the observations made above that all seven PαMS-PS diblock copolymers synthesized in this study are *homogeneous*, which is consistent with the results of DSC measurements and predictions based on Helfand–Wasserman's theory (see Table III).

Plateau Modulus of PαMS-PS Diblock Copolymers. We have shown in Figures 10, 14, 15, 17, and 19–21 that the PαMS-PS block copolymer samples synthesized in this study do not exhibit a distinct plateau value for G'_r. It is suggested in the literature[40] that the plateau modulus $G°_N$ of an entangled polymer can be calculated from measurements of dynamic loss modulus G'', using the following expression:

$$G°_N = \frac{2}{\pi}\int_{-\infty}^{a} G''(\omega)\, d\ln\omega \tag{10}$$

where a is the upper limit for the terminal peak of G''. However, owing to the practical difficulty with identifying the upper limit a of the integral appearing in eq 10 (see Figures 10, 14, 15, 17, and 19–21), in this study we have determined values of $G°_N$ for the block copolymers, using the procedure described in reference to Figure 12.

Figure 22 gives plots of $G°_N$ versus weight fraction of PαMS in the seven PαMS-PS diblock copolymers synthesized in this study. It should be mentioned that the values of $G°_N$ for homopolymers PαMS and PS used in Figure 22 are taken from the literature,[40] because the molecular weights of the homopolymers PαMS and PS that we synthesized in the present study were not sufficiently large, which can give rise to values of $G°_N$ that become independent of molecular weight. It can be seen in Figure 22 that the plateau modulus of PαMS-PS diblock copolymer determined in this study monotonically increases with increasing weight fraction of PαMS and that it shows negative deviations from linearity. Also plotted in Figure 22 are the predictions of $G°_N$ made by the following expressions:

$$G°_N = [w_1 G°_{N1}{}^{1/3.4} + w_2 G°_{N2}{}^{1/3.4}]^{3.4} \tag{11}$$

and

$$G°_N = [w_1 G°_{N1}{}^{1/2} + w_2 G°_{N2}{}^{1/2}]^2 \tag{12}$$

It can be seen in Figure 22 that eqs 11 and 12 give almost the same prediction, because the difference in $G°_{Ni}$ (i = 1, 2) for homopolymers PαMS and PS are rather small. It should be mentioned at this juncture that the composition dependence of the plateau modulus for *homogeneous* PαMS-PS diblock copolymers is very similar to that observed for *compatible* binary blends.[41-43]

Theoretical Considerations

In 1975 four research groups[5,6,44-46] published, independently, interesting papers which dealt with the dynamics of *homogeneous* block copolymers, by modifying or extending the bead–spring model of Rouse[47] and Zimm.[48] Hansen and Shen[5] computed the retardation time spectrum of block copolymers, by introducing into the equations of motion a frictional coefficient matrix for dissimilar segments in the block copolymers and then numerically solved for the eigenvalue spectrum. Wang and DiMarzio[44] considered the viscoelasticity of block copolymer solutions in the free-draining limit by modifying the Rouse theory and obtained a numerical solution to the eigenvalue problem. They concluded that the calculated viscoelastic properties for the diblock copolymer were nearly the same as those from the Rouse theory, while the calculated properties for the triblock copolymers were found to deviate from those of the Rouse theory. By modifying the Rouse theory, Hall and DeWames[46] also calculated the relaxation spectrum of block copolymers, with the assumption that every block is free draining. Stockmayer and Kennedy[6] considered the continuous limit of the bead–spring model of Rouse (i.e., free-draining case) to study the chain dynamics of block copolymer molecules. They computed the terminal relaxation time for AB-type diblock and ABA-type triblock copolymers. It should be mentioned that although the Hansen–Shen theory[5] and the Stockmayer–Kennedy theory[6] give equivalent results for the eigenvalues of the characteristic equation, the Stockmayer–Kennedy theory requires the solution of a transcendental equation, whereas the Hansen–Shen theory requires the solution of a matrix equation. Since the solution of the matrix equation requires more computational effort and the eigenvalues determined from a modified Rouse matrix may depend on the number of elements in the matrix chosen for computation, it is much easier to apply the Stockmayer–Kennedy theory than the Hansen–Shen theory.

In this section we will first review very briefly the Stockmayer–Kennedy theory which in its present form can be used to predict the linear viscoelastic properties of low molecular weight homogeneous block copolymers. We will then modify the Stockmayer–Kennedy theory to predict the linear viscoelastic properties of *entangled* homogeneous block copolymers, by incorporating the concept of the tube model of Doi and Edwards.[49] Finally, we will compare predictions, based on the *modified* Stockmayer–Kennedy theory, of zero-shear viscosities of PαMS-PS diblock copolymers with experimental results.

The Stockmayer–Kennedy Theory. Stockmayer and Kennedy[6] studied the chain dynamics of a homogeneous AB- or ABA-type block copolymer by considering the continuous limit of the bead–spring model of Rouse:

$$\frac{\partial x}{\partial t} = (2/\tau_1\pi^2)\frac{\partial^2 x}{\partial s^2} \tag{13}$$

where x denotes the average displacement of a bead, s is the continuous variable that lies between −1 and 1 (i.e., $-1 \le s \le 1$), and τ_1 is the terminal relaxation time of the homogeneous Rouse chain

$$\tau_1 = N^2 \zeta b^2 / 6\pi^2 k_B T \tag{14}$$

where N is the number of submolecules, ζ is the friction coefficient of the chain segment, b^2 is the mean-square end-to-end length of a submolecule, k_B is the Boltzmann constant, and T is the absolute temperature. They obtained the general solution:

$$x_B = \exp(-t/2\tau)(C_B \sin \beta s + D_B \cos \beta s) \tag{15a}$$

$$x_A = \exp(-t/2\tau)(C_A \sin \alpha s + D_A \cos \alpha s) \tag{15b}$$

where

$$\tau = \tau_{1A}(\pi/2\alpha)^2 = \tau_{1B}(\pi/2\beta)^2 \tag{16}$$

in which τ_{1A} and τ_{1B} are the terminal relaxation times for block A and block B, respectively.

By applying the following boundary conditions to eq 15:

$$K_A \left(\frac{\partial x_A}{\partial s} \right)_{s=\theta} = K_b \left(\frac{\partial x_B}{\partial s} \right)_{s=0} \tag{17a}$$

$$x_A(\theta,t) = x_B(\theta,t) \tag{17b}$$

$$(\partial x(s,t)/\partial s)_{s=\pm 1} = 0 \tag{17c}$$

where $K_A = 3k_BT/b_A{}^2$, $K_B = 3k_BT/b_B{}^2$, and θ is the fractional volume of block B, Stockmayer and Kennedy calculated for an AB-type diblock or an ABA-type triblock copolymer the eigenvalues α that satisfy the characteristic equation

$$\tan\,[\alpha(1-\theta)] = -\lambda\mu \tan \alpha\lambda\theta \quad \text{(even modes)} \tag{18a}$$

$$= \lambda\mu \cot \alpha\lambda\theta \quad \text{(odd modes)} \tag{18b}$$

where

$$\lambda = (\tau_{1B}/\tau_{1A})^{1/2} \qquad \mu = (b_A/b_B)^2 \tag{19}$$

and constructed generalized plots for *reduced* viscosity for a block copolymer, F, defined by

$$F = \frac{\sum_{p=1}^{N} \tau_{p,\text{block}}}{(1-\theta)\sum_{p=1}^{N} \tau_{p,A} + \theta \sum_{p=1}^{N} \tau_{p,B}} \tag{20}$$

where $\tau_{p,A}$ and $\tau_{p,B}$ are the relaxation times for block A and block B, respectively, and $\tau_{p,\text{block}}$ are the relaxation times for the block copolymer. Note that for an ABA-type triblock copolymer $\Sigma\tau_{p,\text{block}}$ must be determined from

$$\sum \tau_{p,\text{block}} = \tau_{1,A}(\pi/2)^2 \sum_{\substack{p \\ \text{all}}}^{N} 1/\alpha_p{}^2 \tag{21}$$

and for an AB-type diblock copolymer $\Sigma\tau_{p,\text{block}}$ must be determined from

$$\sum \tau_{p,\text{block}} = \tau_{1,A}\pi^2 \sum_{\substack{p \\ \text{even}}}^{N} 1/\alpha_p{}^2 \tag{22}$$

Note in eqs 21 and 22 that $\tau_{1,A}$ is the terminal relaxation time for block A and the summation must be taken over all integer values (for both even and odd modes of the characteristic equation, eq 18) for an ABA-type triblock copolymer, and only over even integer values (i.e., for only even modes of the characteristic equation, eq 18a) for an AB-type block copolymer.

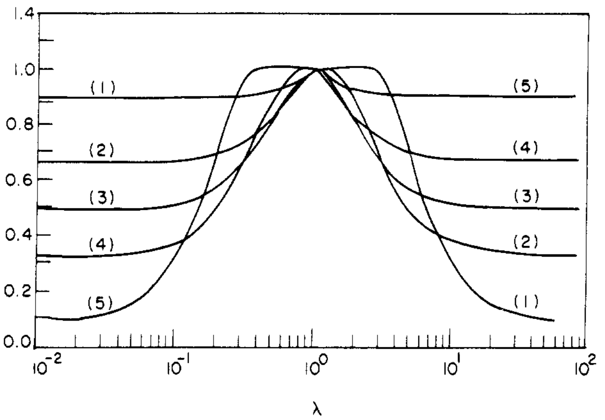

Figure 23. Plots of F versus λ for AB-type diblock copolymers having the same Kuhn statistical length ($\mu = 1$) for various values of block length ratio (θ): (1) $^1/_{10}$; (2) $^1/_3$; (3) $^1/_2$; (4) $^2/_3$; (5) $^9/_{10}$.

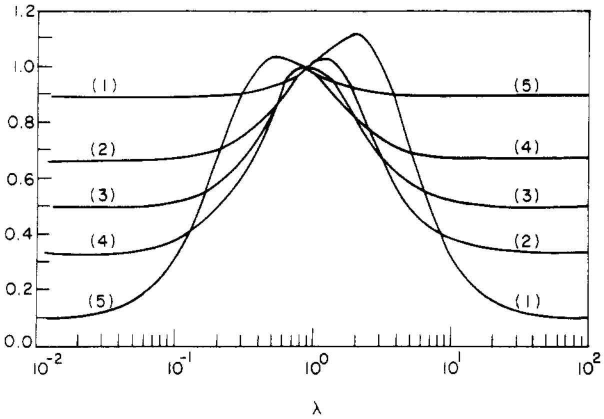

Figure 24. Plots of F versus λ for AB-type diblock copolymers with $\mu = 1.15$ for various values of block length ratio (θ): (1) $^1/_{10}$; (2) $^1/_3$; (3) $^1/_2$; (4) $^2/_3$; (5) $^9/_{10}$.

Let us briefly look at the prediction of reduced viscosity F, defined by eq 20, for AB-type diblock and ABA-type triblock copolymers, respectively, in terms of three important molecular parameters, namely, the Kuhn statistical lengths, the terminal relaxation times of the constituent blocks, and block length ratio θ. Figure 23 gives plots of F versus λ, for an AB-type block copolymer at various values of θ, when the Kuhn statistical lengths of the constituent blocks are the same (i.e., $\mu = 1$). Notice that θ is the fractional volume of block B. It is of interest to observe in Figure 23 that all curves pass through the same point at $\lambda = 1$ and $F = 1$. Notice that $F(\lambda,\theta) = F(1/\lambda,1-\theta)$ as it should be for a diblock copolymer. However, as can be seen in Figure 24, when $\mu \neq 1$, curves for different values of θ do not pass through a common point at $\lambda = 1$. A comparison of Figure 24 with Figure 23 indicates that F is very sensitive to small differences in the statistical lengths between the constituent blocks. Also, for $\mu \neq 1$, $F(\lambda,\theta)$ is no longer the same as $F(1/\lambda,1-\theta)$.

Figure 25 gives plots of F versus λ for an ABA-type triblock copolymer with $\mu = 1.15$ corresponding to the α-methylstyrene/styrene pair, at various values of θ. It is of interest to observe in Figure 25 that (1) when $\lambda < 1$ (i.e., when $\tau_A > \tau_B$), the F is greater than 1 for all values of θ and the relaxation time of endblock A controls the viscosity

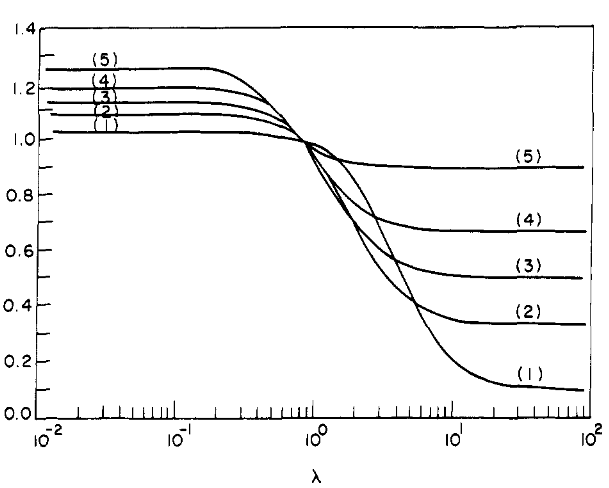

Figure 25. Plots of F versus λ for ABA-type triblock copolymers with $\mu = 1.15$ for various values of block length ratio (θ): (1) $^1/_{10}$; (2) $^1/_3$; (3) $^1/_2$; (4) $^2/_3$; (5) $^9/_{10}$.

of an ABA-type triblock copolymer, and (2) when $\lambda > 1$ (i.e., when $\tau_B > \tau_A$), the F is less than 1 for all values of θ and the relaxation time of midblock B controls the viscosity of an ABA-type triblock copolymer. It should be pointed out that for a given block copolymer or a given value of θ, a variation of λ can come from different sensitivities of relaxation time or viscosity of each block to temperature. It should be noted that λ is also dependent upon θ. Such plots as those given in Figures 23–25 will be very useful to the design of homogeneous block copolymers with desired values of zero-shear viscosity $\eta_{0,\text{block}}$. Specifically, when the block length ratio of a block copolymer (ϕ) is specified and also information on the zero-shear viscosities of the constituent components, $\eta_{0,A}$ and $\eta_{0,B}$, for the specified molecular weights is available, using Figures 23–25 the zero-shear viscosity of the block copolymer, $\eta_{0,\text{block}}$, can be calculated from

$$\eta_{0,\text{block}} = F\{(1-\phi)\eta_{0,A}r_{M,A} + \phi\eta_{0,B}r_{M,B}\} \qquad (23)$$

where $r_{M,A} = M_{e,A}/M_{e,\text{block}}$ and $r_{M,B} = M_{e,B}/M_{e,\text{block}}$ for entangled polymers, but $r_{M,A} = M_A/M_{\text{block}} = 1-\phi$ and $r_{M,B} = \phi$ for unentangled polymers. Note that $M_{e,A}$ and $M_{e,B}$ are the entanglement molecular weights of the constituent components A and B, respectively, and $M_{e,\text{block}}$ is the entanglement molecular weight of the block copolymer, which can be evaluated using an appropriate mixing rule.

Modification of the Stockmayer–Kennedy Theory for Entangled Block Copolymers. As pointed out above, since the Stockmayer–Kennedy theory is based on the Rouse model, the theory in its present form is applicable only to low molecular weight block copolymer melts. In view of the fact that either one or both blocks in the seven PαMS-PS diblock copolymers used in our experiment are greater than the entanglement molecular weight(s) of the corresponding homopolymer(s), we modified the Stockmayer–Kennedy theory as described below. Note that the M_e of PαMS is reported to be about 13 500 and the M_e of PS is about 18 000.[18]

In this study, using the concept of the tube model,[49] we calculated the zero-shear viscosities of the PαMS-PS diblock copolymers that we have synthesized from

$$\eta_{0,\text{block}} = \frac{8}{\pi^2}\frac{\rho RT}{M_{e,\text{block}}}\sum_{p=1}^{N}\tau_{p,\text{block}} \qquad (24)$$

where ρ is the density of the block copolymer which depends on temperature, R is the gas constant, and $\sum\tau_{p,\text{block}}$ is defined by eq 22. It should be mentioned that according to the tube model, the zero-shear viscosity of a homopolymer, η_0, is given by

$$\eta_0 = \frac{8}{\pi^2}\frac{\rho RT}{M_e}\sum_{\substack{p\\ \text{odd}}}^{\infty}\frac{1}{p^2}\tau_p \qquad (25)$$

where $\tau_p = \tau_1/p^2$, τ_1 being the terminal relaxation time. Notice that eq 24 is not quite the same as eq 25 in that the summation in eq 24 is taken over all integer values, whereas the summation in eq 25 is taken only over odd integer values. When the molecular weights of both PαMS and PS blocks were *greater* than the entanglement molecular weights of corresponding homopolymers (samples BII, CI, CII, CIII, and CIV), we calculated the terminal relaxation time $\tau_{1,i}$ (i = PαMS, PS) of the constituent blocks, using the tube model[49]

$$\tau_{1,i} = 12\eta_{0,i}M_{e,i}/\pi^2\rho RT \qquad (26)$$

where $\eta_{0,i}$ is the zero-shear viscosity of homopolymer PαMS or homopolymer PS having the same molecular weight as in the PαMS-PS diblock copolymer, and $M_{e,i}$ is the entanglement molecular weight of homopolymer PαMS or homopolymer PS. However, when the molecular weight of either PαMS block or PS block was *less* than the M_e of the corresponding homopolymer (samples CV and CVI), we calculated its terminal relaxation time using the Rouse model[47]

$$\tau_{1,i} = 6\eta_{0,i}M_i/\pi^2\rho RT \qquad (27)$$

Note that the terminal relaxation times defined by eq(s) 26 and/or 27 are needed in order to calculate eigenvalues α by solving eq 18.

Since information on $M_{e,\text{P}\alpha\text{MS/PS}}$ was not available, we used the following expression:

$$M_{e,\text{P}\alpha\text{MS/PS}} = \rho RT/G^\circ_{N,\text{P}\alpha\text{MS/PS}} \qquad (28)$$

where $G^\circ_{N,\text{P}\alpha\text{MS/PS}}$ is the plateau modulus of the PαMS-PS diblock copolymer, which in this study was estimated from eq 11.

Comparison of Prediction with Experiment. We used $\eta_{0,\text{P}\alpha\text{MS}} = 1.1 \times 10^5$ Pa s at 230 °C for PαMS-100 having $M_w = 9.8 \times 10^4$ to calculate, with the aid of $\eta_0 \propto M^{3.4}$, the zero-shear viscosities of the PαMS blocks in samples BII, CI, CII, CIII, CIV, and CV and to calculate, with the aid of $\eta_0 \propto M$, the zero-shear viscosity of the PαMS block in sample CVI. And we used $\eta_{0,\text{PS}} = 1.62 \times 10^3$ Pa s at 230 °C for PS having $M_w = 1.95 \times 10^5$ to calculate, with the aid of $\eta_0 \propto M^{3.4}$, the zero-shear viscosities of the PS blocks in samples BII, CI, CII, CIII, CIV, and CVI and to calculate, with the aid of $\eta_0 \propto M$, the zero-shear viscosity of PS block in sample CV. It should be mentioned that earlier Fujimoto et al.[16] reported $\eta_{0,\text{P}\alpha\text{MS}} = 2.16 \times 10^8$ Pa s at 186 °C for PαMS having $M_w = 9.1 \times 10^4$. Using $\eta_0 \propto M^{3.4}$ and the WLF equation, from Fujimoto's data, we obtain $\eta_{0,\text{P}\alpha\text{MS}} = 5.1 \times 10^4$ Pa s at 230 °C for $M_w = 9.8 \times 10^4$. We found that the value of $\eta_{0,\text{P}\alpha\text{MS}}$ determined by Fujimoto is one half of that obtained in the present study.

A summary of the comparison between predicted and experimental values of $\eta_{0,\text{block}}$ for the seven PαMS-PS block copolymers investigated are given in Table IV. It should be mentioned that the experimental values of $\eta_{0,\text{block}}$ given in Table IV were determined using the relationship, $\eta_0 = \lim_{\omega\to 0} G''(\omega)/\omega$.

In order to observe the effect of block copolymer composition on $\eta_{0,\text{block}}$, we calculated values of $\eta_{0,\text{block}}$ with the total molecular weight reduced to a reference molec-

Table IV
Comparison of Prediction with Experimental Results for $\eta_{0,\mathrm{block}}$ of PαMS-PS Diblock Copolymer at 230 °C

sample code	measured $\eta_{0,\mathrm{block}}$, Pa s	predicted $\eta_{0,\mathrm{block}}$, Pa s
BII	1.3×10^4	2.8×10^3
CI	1.4×10^4	2.5×10^3
CII	1.5×10^5	2.3×10^4
CIII	2.0×10^5	1.1×10^5
CIV	1.2×10^4	2.1×10^3
CV	2.8×10^5	2.4×10^5
CVI	6.5×10^3	1.4×10^3

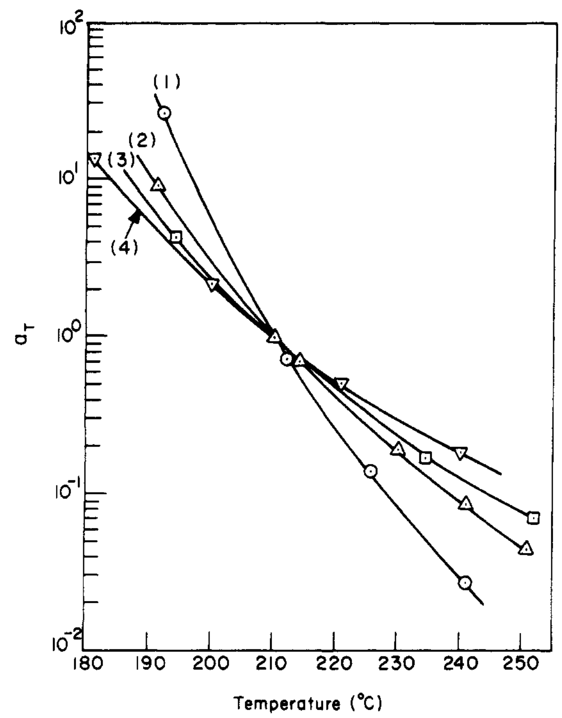

Figure 26. Plots of log a_T versus temperature for sample CV (⊙), sample CII (▲), sample CIV (▣), and sample CVI (▼), where solid curves describe the predictions made with the WLF equation.

ular weight of 2.0×10^5 at 230 °C. For this, we used $\eta_0 \propto M^{3.4}$ and the WLF equation[18]

$$\log a_T = \frac{-c_1(T - T_o)}{c_2 + T - T_o} \qquad (29)$$

Using the following numerical values: (a) $c_1 = 8.86$, $c_2 = 101.6$, and $T_o = 204$ °C for PαMS;[16] and (b) $c_1 = 13.7$, $c_2 = 50$, and $T_o = 100$ °C for PS,[18] we obtained the viscosity shift factor a_T for each of the seven PαMS-PS diblock copolymers investigated, and plots of a_T versus temperature are given in Figure 26. It can be seen in Figure 26 that the temperature dependence of the shift factor a_T varies with block length ratio, owing to a large difference in glass transition temperature T_g between PαMS and PS. Figure 27 gives a comparison of predicted and experimental results of $\eta_{0,\mathrm{block}}$ for PαMS-PS diblock copolymers with molecular weights reduced to a reference molecular weight of 2.0×10^5. Note in Figure 27 that the dotted curve is drawn through the data points and the vertical bars on the data points indicate the range of error that would be incurred when there was 5% error in the determination of molecular weight.

It can be seen in Table IV and Figure 27 that agreement between experiment and prediction made with the modified Stockmayer–Kennedy theory is good for sample CV, which has 83 wt % of PαMS, and that the difference between experiment and prediction becomes greater as the amount of PαMS in the block copolymer decreases. It should be mentioned that at equal molecular weight, the viscosity of PαMS is much greater than (about 500 times) that of PS at 230 °C. This then suggests that the PαMS block in a PαMS-PS diblock copolymer plays a predominant role over the PS block, in controlling the viscosity of the block copolymer. Notice, however, that in the modified Stockmayer–Kennedy theory we treated the PαMS block as a Rouse chain (thus, $\eta_{0,\mathrm{P\alpha MS}} \propto M$) when the molecular weight of PαMS block is less than its entanglement molecular weight. It is quite clear from Figure 27 that such an approach greatly underestimates the contribution of the PαMS block to the $\eta_{0,\mathrm{block}}$ of the entire block copolymer.

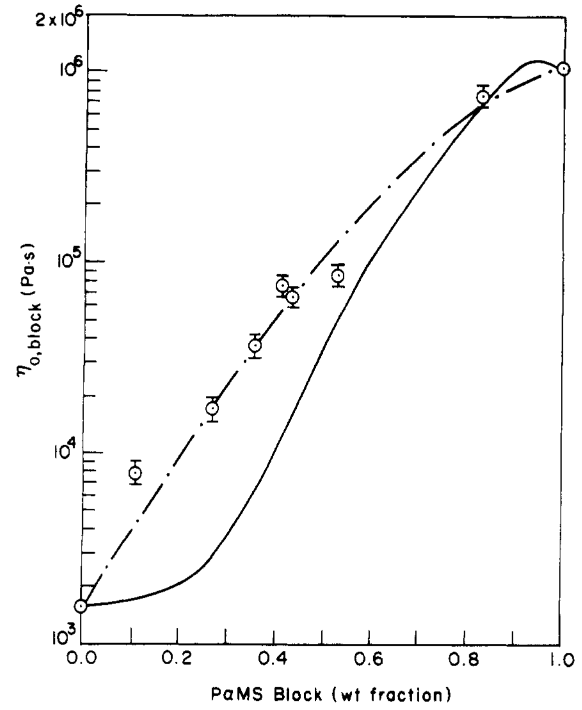

Figure 27. Plots of log $\eta_{0,\mathrm{block}}$ versus weight fraction of PαMS block for the PαMS-PS diblock copolymers synthesized in this study, where the solid line is a prediction by the modified Stockmayer–Kennedy theory, and the dotted line is drawn as a guide through the experimental data. Reference molecular weight used is 2×10^5 and reference temperature used is 230 °C.

We are well aware of the fact that when considering the dynamics of a block copolymer having molecular weight greater than the entanglement molecular weight of the constituent blocks with a tube-model approach, we must treat both PαMS and PS blocks as *a single chain* with the cooperative reptation motion in a tube, instead of evaluating values of the relaxation times for the PαMS and PS blocks separately. However, before attacking the problem using a tube-model approach, a number of fundamental questions must first be answered. Some of those questions are as follows: (a) How important are the hydrodynamic interactions between the constituent blocks? (b) What role does the extent of thermodynamic compatibility between the constituent blocks play? (c) What is the appropriate expression for an external potential? (d) Will the use of a mean-field approach be acceptable if one wishes to use it? (e) How should we treat the cooperative relaxation motion of a block copolymer with information on the relaxation motions of the constituent blocks? These are by no means trivial questions, and at present we are pursuing to answer some of those questions.

Concluding Remarks

In the present study, we synthesized seven PαMS-PS diblock copolymers with block molecular weights ranging from 1.2×10^5 to 2.5×10^5, and with widely different block length ratios. Note that these block copolymers are regarded as *entangled* in the molten state. We confirmed that these block copolymers contained *no* microdomains (i.e., homogeneous), using DSC and, also, logarithmic plots of dynamic storage modulus and dynamic loss modulus. In taking rheological measurements of the block copolymers, we used an antioxidant to avoid possible degradation of the sample during the experiments. Our rheological measurements have revealed that the melt elasticity, as interpreted with log G' versus log G'' plots, is dependent upon block length ratio, but independent of the total molecular weight for a constant block length ratio.

In the present study we have modified, on an ad hoc basis, the Stockmayer–Kennedy theory, that was developed originally for homogeneous low molecular weight (i.e., *unentangled*) block copolymer melts, in order to predict zero-shear viscosities of the *entangled* PαMS-PS diblock copolymers that we synthesized. We have found that the modified Stockmayer–Kennedy theory underestimates the contribution of the PαMS block to the zero-shear viscosity of the PαMS-PS diblock copolymer when the PαMS block becomes a minor constituent component. We have pointed out an urgent need for developing a molecular viscoelasticity theory for homogeneous, entangled block copolymers.

It should be mentioned that although in this paper our concern was confined to the rheological behavior of homogeneous block copolymers, a better understanding of the rheological behavior of microphase-separated block copolymers is equally important from both fundamental and practical points of view. At present, there exists no theory, which enables us to predict the rheological behavior of microphase-separated block copolymers in terms of molecular parameters (i.e., block molecular weights and block length ratio) and microdomain morphology. This is an important and challenging research area for polymer scientists.

References and Notes

(1) Robeson, L. M.; Matzner, M.; Fetters, L. J.; McGrath, J. E. In *Recent Advances in Polymer Blends, Grafts and Blocks*; Sperling, L. H., Ed.; Plenum Press: New York, 1974; p 281.
(2) Dunn, D. J.; Krause, S. *J. Polym. Sci., Polym. Lett. Ed.* **1974**, *12*, 591.
(3) Krause, S.; Dunn, D. J.; Seyed-Mozzaffari, A.; Biwas, A. M. *Macromolecules* **1977**, *10*, 786.
(4) Hansen, D. R.; Shen, M. *Macromolecules* **1975**, *8*, 903.
(5) Hansen, D. R.; Shen, M. *Macromolecules* **1975**, *8*, 343.
(6) Stockmayer, W. H.; Kennedy, J. W. *Macromolecules* **1975**, *8*, 351.
(7) Hellstern, A. M.; DeSimone, J. M.; McGrath, J. E. *Polym. Prepr., Am. Chem. Soc., Div. Polym. Chem.* **1988**, *29* (2), 342.
(8) Kim, J. K. Molecular Aspects of Viscoelasticity of Compatible Polymer Blends and Block Copolymers. Doctoral Dissertation, Polytechnic University, Brooklyn, NY, 1990.
(9) Morton, M.; Fetters, L. J. *Rubber Chem. Technol.* **1975**, *48*, 359.
(10) Lau, S. F.; Pathak, J.; Wunderlich, B. *Macromolecules* **1982**, *15*, 1278.
(11) Saeki, S.; Cowie, J. M. G.; McEwen, I. J. *Polymer* **1983**, *24*, 60.
(12) Widmaier, J. M.; Mignard, G. *Eur. Polym. J.* **1987**, *23*, 989.
(13) Lin, J. L.; Roe, R. J. *Polymer* **1988**, *29*, 1227.
(14) Schneider, H. A.; Cantow, H. J.; Wendland, C.; Leikauf, B. *Makromol. Chem.* **1990**, *191*, 2377.
(15) Fox, T. G. *Bull. Am. Phys. Soc.* **1956**, *1*, 123.
(16) Fujimoto, T.; Ozaki, N.; Nagasawa, M. *J. Polym. Sci., Part A-2* **1968**, *6*, 129.
(17) Odani, H.; Nemoto, N.; Kitamura, S.; Tamura, M. *Polym. J.* **1970**, *1*, 356.
(18) Ferry, J. D. *Viscoelastic Properties of Polymers*, 3rd ed.; Wiley: New York, 1980; p 330.
(19) Phalip, P.; Favier, J. C.; Sigwalt, P. *Polym. Bull.* **1984**, *12*, 331.
(20) Suzuki, H.; Miyamoto, Y. *Macromolecules* **1990**, *23*, 1877.
(21) Cowie, J. M. G.; Bywater, S. *J. Polym. Sci.* **1961**, *54*, 221.
(22) Braun, D.; Heufer, G. *Makromol. Chem.* **1964**, *79*, 98.
(23) Leibler, L. *Macromolecules* **1980**, *13*, 1602.
(24) Meier, D. J. In *Thermoplastic Elastomers*; Legge, N. R., Holden, G., Schroeder, H., Eds.; Hanser: New York, 1987; Chapter 11.
(25) Helfand, E.; Wasserman, Z. W. *Macromolecules* **1976**, *9*, 879; *Polym. Eng. Sci.* **1977**, *17*, 535; *Macromolecules* **1980**, *13*, 994; In *Development in Block Copolymers*; Goodman, I., Ed.; Applied Science: New York, 1982; Chapter 3.
(26) Lin, J. L.; Roe, R. J. *Macromolecules* **1987**, *20*, 2168.
(27) Richardson, M. J.; Savill, N. G. *Polymer* **1977**, *18*, 3.
(28) Cowie, J. M. G.; Toporowski, P. M. *J. Macromol. Sci.-Phys.* **1969**, *B3*, 81.
(29) Colby, R. H.; Fetters, L. J.; Graessley, W. W. *Macromolecules* **1987**, *20*, 2226.
(30) Han, C. D.; Kim, J. *J. Polym. Sci., Part B: Polym. Phys. Ed.* **1987**, *25*, 1741.
(31) Kraus, G.; Rollmann, K. W. *J. Appl. Polym. Sci.* **1977**, *21*, 3311.
(32) Han, C. D.; Lem, K. W. *Polym. Eng. Rev.* **1983**, *2*, 135.
(33) Chuang, H. K.; Han, C. D. *J. Appl. Polym. Sci.* **1984**, *29*, 2205.
(34) Han, C. D.; Jhon, M. S. *J. Appl. Polym. Sci.* **1986**, *32*, 3809.
(35) Han, C. D.; Yang, H. H. *J. Appl. Polym. Sci.* **1987**, *33*, 1199.
(36) Kim, J.; Han, C. D.; Chu, S. G. *J. Polym. Sci., Part B: Polym. Phys.* **1988**, *26*, 677.
(37) Han, C. D.; Kim, J.; Kim, J. K. *Macromolecules* **1989**, *22*, 383.
(38) Han, C. D.; Baek, D. M.; Kim, J. K. *Macromolecules* **1990**, *23*, 561.
(39) Han, C. D.; Kim, J.; Baek, D. M.; Chu, S. G. *J. Polym. Sci., Part B: Polym. Phys.* **1990**, *28*, 315.
(40) Graessley, W. W. *Adv. Polym. Sci.* **1974**, *16*, 1.
(41) Wu, S. *J. Polym. Sci., Polym. Phys.* **1989**, *27*, 723; *Polymer* **1987**, *28*, 1144.
(42) Composto, R. J. Diffusion in Polymer Blends. Doctoral Dissertation, Cornell University, Ithaca, NY, 1987.
(43) Han, C. D.; Kim, J. K. *Macromolecules* **1989**, *22*, 4292.
(44) Wang, F. W.; DiMarzio, E. A. *Macromolecules* **1975**, *8*, 356.
(45) Wang, F. W. *Macromolecules* **1975**, *8*, 364.
(46) Hall, W. F.; DeWames, R. E. *Macromolecules* **1975**, *8*, 349.
(47) Rouse, P. E. *J. Chem. Phys.* **1953**, *21*, 1272.
(48) Zimm, B. H. *J. Chem. Phys.* **1956**, *24*, 269.
(49) Doi, M.; Edwards, S. F. *The Theory of Polymer Dynamics*; Clarendon: Oxford, 1986.

Registry No. PαMS–PS (block copolymer), 108080-90-6.